Master's thesis

NTNU
Norwegian University of Science and Technology
Faculty of Engineering
Department of Energy and Process Engineering

Dorthea Vollset Almklov

Trans-Arctic re-routing of container vessels using the MariTEAM model

A comparative analysis of short- and long-term climate change impacts

Master's thesis in Industrial Ecology
Supervisor: Anders Hammer Strømman
Co-supervisor: Diogo Kramel
June 2022

NTNU
Norwegian University of
Science and Technology

Dorthea Vollset Almklov

Trans-Arctic re-routing of container vessels using the MariTEAM model

A comparative analysis of short- and long-term climate change impacts

Master's thesis in Industrial Ecology
Supervisor: Anders Hammer Strømman
Co-supervisor: Diogo Kramel
June 2022

Norwegian University of Science and Technology
Faculty of Engineering
Department of Energy and Process Engineering

NTNU
Norwegian University of
Science and Technology

Thesis description

As part of the KPN research project CLIMMS (Climate change mitigation in the maritime sector), NTNU has developed a computational model for the fuel combustion and emissions to air from the global shipping fleet; the MariTEAM model. The model uses historical AIS (automatic identification system, i.e., ship location data) in combination with weather data, and ship technical data. The master thesis will be performed in co-operation with the CLIMMS project and will contribute with expanding the model to include a feature that will enable re-routing of ships.
The objective of the master thesis is to establish a routine for modifying the operational profile of a sub-set of ships from the global fleet. As less sea ice in the Arctic is inviting more shipping activities, this thesis will explore the effects of rerouting ships travelling from Asia to Europe from the Suez Canal through the Arctic. Changing routes to go through the Arctic could reduce travel times and hence greenhouse gas and pollution emissions if travelling from e.g., China to Europe. Yet more direct emissions in the Arctic could be derogative to the local environment. This master will explore how emissions are changing with such changes in shipping activities through the use of MariTEAM.

The following tasks are to be considered:

1. Selection of a suitable sub-selection of ships to study.
2. Development of a logical routine for altering the routes and changing the operational profile of the ships.
3. Run the MariTEAM model with and without rerouting.
4. Analysis of the output of the model to establish effects of travelling through Arctic rather than Suez.

Supervisor: Anders Hammer Strømman
Co-supervisors: Helene Muri, Diogo Kramel.

The student will have licenced access to the following software and data for the duration of the work: The MariTEAM ship emission model and its database dependencies: Sea-Web, AIS data, and weather data.

Abstract

Maritime shipping is responsible for 80% of global trade volume, and as demand is expected to increase, so are the exhaust emissions associated with vessel activity. The Arctic region warms twice as fast as the global average. The projected decrease in ice extent and thickness opens the possibility for Trans-Arctic shipping as a shorter alternative to conventional Eurasian trade routes on the Suez Canal Route (SCR). The State-of-the-art, bottom-up emission assessment model "MariTEAM" is modified to establish a rerouting routine and simulate five Maersk container vessels through the Suez Canal Route and the Northern Sea Route (NSR). The aim is to assess the climate change mitigation potential of rerouting vessels through the Arctic given technical ship data, operational profiles, and fuel profiles. Two dual simulations are conducted where the container ships are simulated through the Arctic with (1) constant speed equal to the average speed on the SCR and (2) constant slow steaming speed.

Results from a climate impact assessment using GWP and GTP metrics indicate that vessels run on heavy fuel oil (HFO) have minimal short-term climate change mitigation potential of rerouting due to the cooling effect of sulfur. Further, the case vessels are assessed with marine diesel oil (MDO) fuel on the NSR to simulate an Arctic HFO-ban. The case vessels are also simulated with liquified natural gas (LNG) as fuel to assess the potential climate change mitigation of rerouting in a scenario where HFO is being phased out as marine fuel. Due to cooling NOx emissions, short-term temperature potential is a net negative for all experiments. The long-term climate change mitigation of rerouting is present for all fuel profiles and operational profiles, as the navigational distance reduction on the NSR leads to reduced fuel consumption and emissions of long-lived GHGs. Long-term trade-offs regarding rerouting through the NSR are increased local warming, potentially amplifying permafrost thawing, and affecting biodiversity.

Sammendrag

Maritim skipsfart står for 80 % av verdenshandelen i volum, og ettersom etterspørselen forventes å øke, vil også eksosutslippene knyttet til fartøysaktivitet øke. Arktis varmes opp dobbelt så raskt som det globale gjennomsnittet, og anslått reduksjon i isens utbredelse og tykkelse åpner muligheten for transarktisk skipsfart som et kortere alternativ til konvensjonelle eurasiske handelsruter på Suezkanalruten (SCR). Den toppmoderne utslippsvurderingsmodellen "MariTEAM" er modifisert for å etablere en omrutingsrutine, og ytterligere simulere fem Maersk-containerskip gjennom Suezkanalruten og den Nordlige sjørute (NSR). Målet er å vurdere potensialet for å redusere klimapåvirkningen av sjøfartøy, ved å omdirigere fartøyer gjennom NSR, gitt tekniske skipsdata, operasjonelle profiler og drivstoffprofiler. To dobbel-simulering-eksperimenter er utført hvor fartøyene simuleres gjennom Arktis med (1) konstant hastighet lik gjennomsnittshastigheten på SCR og (2) konstant redusert speed, også kjent som «slow steaming».

Resultater fra en klimakonsekvensvurdering ved bruk av GWP- og GTP-målinger indikerer at fartøyer som kjøres på tung fyringsolje (HFO) har minimalt potensial for å redusere klimaendringer på kort sikt grunnet kjøleeffekten av svovel. Videre vurderes casefartøyene med marin dieselolje (MDO) som drivstoff på NSR for å simulere et Arktisk HFO-forbud. Case-fartøyene simuleres også med flytende naturgass (LNG) som drivstoff for å vurdere de potensielle klimaeffektene ved omruting i et scenario der HFO fases ut som marint drivstoff. Kortsiktig temperaturpotensial er netto negativt for alle forsøk på grunn av kjøleeffekten av NO_x-utslipp. På lang sikt er en reduksjon av globale klimapåvirkninger ved omruting til stede for alle drivstoffprofiler og driftsprofiler, ettersom reduksjonen av navigasjonsavstanden på NSR fører til redusert drivstofforbruk og reduserte utslipp av langlevde klimagasser. Langsiktige avveininger angående omruting til NSR er økt lokal oppvarming i Arktis, som mulig kan forsterke tining av permafrost og påvirke biologisk mangfold.

Acknowledgements

This thesis concludes my master's degree in Industrial Ecology at the Norwegian University of Science and Technology (NTNU). It is a continuation of my project thesis written during the spring semester of 2022 at the Department of Energy and Process Engineering (EPT).

I want to express my gratitude to my supervisor Anders Hammer Strømman, for providing valuable guidance throughout the semester. I want to thank my co-supervisor, Helene Muri, for motivating me and pushing me to believe that I can manage Python, and my co-supervisor, Diogo Kramel, for unique expertise on the MariTEAM model. Thank you for always being available for professional discussions. Finally, I would like to thank my fellow students for their motivation and support and my mother and father for providing moral support and feedback on my work.

Table of contents

List of Tables

List of Figures

Abbreviation

AIS = Automatic Identification System

BC = Black carbon

CO = Carbon Monoxide

DWT = Dead Weight Tonnage

EC = Elemental Carbon

ECA = Environmental Control Area

ECMWF = European Center for Medium-Range Weather Forecasts

GHG = Greenhouse gas

GTP = Global Temperature change Potential

GWP = Global Warming Potential

HFO = Heavy Fuel Oil

HP = High-Pressure engine

IMO = International Marine Organization

IPCC = Intergovernmental Panel on Climate Change

LDT = Light Displacement Tonnage

LF = Load factor

LNG = Liquified Natural Gas

LP = Low-Pressure engine

MCR = Maximum Continous Rating

MDO = Marine Diesel Oil

MMSI = Marine Mobile Service Identity

NM = Nautical Miles

NSR = Northern Sea Route

NTNU = Norwegian Univeristy of Scinece and Technology

OC = Organic Carbon

OP = Operational Profile

RF = Radiative Forcing

SCR = Suez Canal Route

SFOC = Specific Fuel Oil Consumption

SLCFs = Short-Lived Climate Forcers

SOG = Speed Over Ground

TEU = Twentyfeet Equivalent Unit

TH = Time Horizon

1 Introduction

Waterborne transportation is the most cost-efficient trade transport mode and is responsible for 80% of World trade in volume (UNCTAD, 2018). This chapter introduces the challenge of decarbonizing the shipping sector, and the interests in and possibilities for re-routing vessels through the Arctic region as an alternative to the conventional Eurasian trade route through the Suez Canal. The chapter is divided into three main sections. Firstly, the background and motivation for studying the topic of Arctic shipping are presented, followed by a section on the state of knowledge about emissions associated with ship exhaust combustion, previous literature assessing emissions from shipping activity, and theoretical knowledge about fuel and emission saving tools. Further, the research objective and report structure are presented.

1.1 Background and motivation

Climate change is a global threat affecting economies and society caused by anthropogenic greenhouse gas (GHG) emissions. In 2015 a legally binding international treaty on climate change was adopted by 196 countries where the goal was set to limit global warming to well below 2℃, preferably to 1.5℃ compared to pre-industrial times (UNFCCC, 2015). This international treaty is known as the Paris Agreement. All countries and sectors require substantial emission mitigation to reach the global temperature goal. One sector that is considered hard to mitigate is the transport sector, which is responsible for 16.2%[1] of global anthropogenic CO_2 emissions (Ritchie & Roser, 2020). Shipping is the most widely used mode of trade transport, accounting for approximately 80% of the World trade by volume in 2018 (UNCTAD, 2018), and is associated with 11% of the anthropogenic transport emissions (Tiseo, 2021), amountig to 1,076 million tons CO_2-equivalents (Faber et al., 2020). *The International Marine Organization* (IMO) has set a goal to cut annual GHG emissions by 40% within 2030 compared to 2008 levels and further work to phase out the GHG emissions from shipping entirely as soon as possible in this century (IMO, n.d,). At the same time, shipping demand is increasing, and the emissions continue to grow accordingly (Faber et al., 2020; Pathak et al., 2021). The Annual Efficiency Ratio (AER) is s metric used by the IMO GHG studies to compare vessels of varied sizes and weights in terms of carbon intensity (Faber et al., 2020; Smith et al., 2015). GHG emissions are divided by deadweight tonnage (DWT) as a proxy

[1] All direct emissions (scope 1) from engine combustion and a small amount of scope 2 emissions from electricity.

for cargo carried and distance sailed over a given period (usually one year) (Parker, Raucci, Smith, & Laffineur, 2015). Although maritime shipping is known for being the most energy-efficient mode of transport in terms of gram CO_2-equivalents per transport work (Myhre et al., 2013b), reaching the goals of the Paris Agreement and the IMO requires a substantial decrease in carbon intensity in the sector.

CO_2 emissions depend on distance sailed, ship size, and vessel speed (Xu & Yang, 2020). The Suez Canal, located in Egypt, connecting the Mediterranean Sea and the Red Sea, is one of the busiest waterways in the world as it historically has served as the shortest transit route from the East to the West (El-Taybany, Moustafa, Mansour, & Tawfik, 2019). The canal has a cargo volume of nearly 80% of Eurasian maritime cargo (Zheng, Xiao, Zhou, Chen, & Chen, 2018). Tankers (27.41%), bulk carriers (27.21%), and container ships (26.56%) were the vessel types with the largest representation through the Suez Canal in 2020, according to Egypt's Suez Canal Authority (SCA) (SCA, n.d,). These vessels are also responsible for the most significant CO_2 emissions worldwide because of their cargo delivery's international and intercontinental nature (Balcombe et al., 2019; Faber et al., 2020). The traffic transiting the Suez Canal cause air pollution (El-Taybany et al., 2019) and has led to congestion and delays, impacting the stakeholders along the supply chain (Lee & Wong, 2021).

Global warming affects the surface temperature differently in different hemispheres. In the Arctic region, the temperature has likely increased by more than double the global surface temperature in the last decade (Fox-Kemper et al., 2021). Ice reflects incoming solar radiation to space. Increased surface temperatures reduces the ice coverage resulting in less reflection and a feedback loop of amplified warming, leading to more rapid sea ice losses (Meredith et al., 2019). The most considerable ice losses in the Arctic are observed in late summer to early autumn (Fox-Kemper et al., 2021). Extended periods of open Arctic waters have increased the interest in Trans-Arctic shipping as an alternative to the busy Suez Canal Route (SCR). The Northern Sea Route (NSR) is a shorter transit route between North-East Asia and Northern Europe, implying lower net CO_2 emissions (H. Lindstad, Bright, & Strømman, 2016; Schøyen & Bråthen, 2011).

On the other hand, the large-scale Arctic warming has triggered increased fires and irreversible thawing of permafrost across the region, which releases GHGs such as carbon dioxide (CO_2) and methane (CH_4) (Lenton et al., 2019). In addition to GHGs, international shipping accounts for 13%

and 12 % of global NO_x and SO_x emissions, respectively (Smith et al., 2015), which are hazardous air pollutants. Their effects on the climate and human health depend on emission location (J. S. Fuglestvedt et al., 2014). Hence, the exhaust emissions from shipping in the Arctic will contribute differently to the global climate impact than the same emissions at lower latitudes.

Most emissions over a ship's life cycle stem from direct exhaust emissions (80-90%), also known as tank-to-wake emissions (Winebrake, Corbett, & Meyer, 2007), which are influenced by the ship's operational profile, the weather, the fuel type, and the power system. Maritime exhaust emissions should thus be assessed using models and simulations of real operational and weather data. The various properties of emission species and the geospatial differences must also be considered in analyzing the climate impact of ship combustion. The following section discusses the state of knowledge related to these aspects and emission reduction strategies of slow steaming and alternative fuels.

1.2 State of knowledge

This section presents previous research and the state of knowledge regarding the atmospheric properties of different emissions species, ship emission modeling, and Arctic shipping. The section serves as the knowledge base for further assumptions and model implications presented in chapters 3 and 4.

1.2.1 Climate forcers and their properties

Exhaust emissions from shipping include long-lived greenhouse gasses (LLGHG) and short-lived climate forcers (SLCF). SLCFs are compounds that either warm or cool the climate over a shorter time than the LLGHGs (Lund et al., 2020). As opposed to CO2, which persists in the atmosphere for decades and centuries, the SLCFs, which include methane, ozone, and aerosols, decay after days or years, depending on the compound (Niak et al., 2021). The different GHGs and SLCFs affect the radiative forcing (RF) in the atmosphere, which is the difference in insolation absorbed by the earth and the solar radiation reflected to space, measured in mWm^{-2} (Myhre et al., 2013b). Some SLCFs, e.g., methane (CH4), carbon monoxide (CO), and black carbon (BC) trap solar radiation and contribute to increasing warming. At the same time, other compounds, e.g., sulfur oxides (SOx) and nitrous oxides (NOx), scatter the incoming solar radiation, which generates a negative radiative forcing, i.e., cooling temperature (Lund et al., 2020). The short atmospheric lifetime of these climate forcers implies that the total RF is related to the emission rate rather than

the cumulative emissions over decades, as for LLGHGs (Collins et al., 2019). The impact of SLCFs are highly location-dependent and can change rapidly if the emission patterns are changed (Niak et al., 2021).

Maritime exhaust emissions are dominated by cooling sulfur oxides (SO_x) and nitrous oxides (NO_x). Despite the short-term net cooling effect on global warming, these aerosols have a hazardous impact on human health (Collins et al., 2019). Due to this, the IMO has implemented regulations to phase out SOx emissions by setting a cap on the mass of sulfur per mass of fuel in ships. The cap was limited to 0.5% sulfur per mass in 2020, from the latest cap of 3.5% in 2012 (IMO, n.d.,-b). Within the IMO's environmental control areas (ECAs), ships are prohibited from using fuel oil with a sulfur content higher than 0.1% per mass (Sun, Yang, & Zheng, 2020). Further, the IMO has introduced NOx emissions regulations limiting ships built or heavily modified after 2000 to a NOx emission factor reduction of approx. 10% (Tier 1), another 15% reduction for newbuilds after 2011 (Tier 2), and a further 75% reduction for newbuilds after 2016 (Tier 3) (IMO, n.d.,-a).

Emission metrics put different emissions on a common scale to compare their climate impact. The most common metric scale is CO2-equivalents, which is obtained by multiplying the magnitude of given emission species by its metric value (J. S. Fuglestvedt et al., 2010; Gasser et al., 2017; Shine, Fuglestvedt, Hailemariam, & Stuber, 2005). Few studies on Arctic shipping have assessed the net impact of emissions in CO2-equivalents.

1.2.2 Tank-to-wake emissions modeling and Arctic shipping

The effective power of a marine engine is the power required to move the vessel forward at a constant speed and is thus a product of speed and resistance (Tezdogan, Incecik, Turan, & Kellett, 2016). Fuel consumption, which determines the emission of CO_2 and SO_x (Faber et al., 2020; Kramel et al., 2021), is not directly derived from effective power. Fuel consumption depends on the engine load, specific fuel oil consumption (SFOC), propulsion speed, and other variables, which all depend on a vessel's different operating conditions (Tezdogan et al., 2016). Simulation models of ship-specific operations have thus been developed to quantify fuel consumption and related maritime transport emissions. Such models are called activity-based or bottom-up models (Nunes, Alvim-Ferraz, Martins, & Sousa, 2017). In contrast, the so-called top-down approach is a simple method that takes a macroeconomic perspective of fuel consumption based on bunker fuel

sales data. This method is believed to underestimate emissions, while the bottom-up approach has proven to provide higher accuracy (Kramel et al., 2021). Bottom-up models include detailed inventories of technical ship details (e.g., identification number, ship type, engine type, and dimensions) and operational data such as service speed, ship tracks, and port calls (Kwon, Lim, Lim, & Lee, 2019; Nunes et al., 2017). For the operational data, the most common source in recent years has been Automatic Identification system data (AIS), which has been required by the IMO since 2004 to be installed on internationally voyaging ships with a Giga tonnage (GT) of 300 or above (IMO, n.d.). The system reports the location of a vessel with a few seconds intervals and has been used by several scholars to describe individual ship operations, which can further be tied to exhaust emissions (Goldsworthy & Goldsworthy, 2015; Johansson, Jalkanen, & Kukkonen, 2017; Smith et al., 2015; Tichavska & Tovar, 2015; Weng, Shi, Gan, Li, & Huang, 2020). Few bottom-up models have included weather data input even though weather and sea state highly affect power output and fuel consumption (Johansson et al., 2017; Tezdogan et al., 2016). The AIS data gives the location and speed of the vessel, which can reflect the weather on the route; however, the *Third IMO GHG Study* assumed that weather effects alone would be responsible for 15% of additional power requirements, accounted for by weather adjustment factors (Smith et al., 2015). These factors were questioned by Johansson et al. (2017) and thus not applied in their Ship Traffic Emission Assessment Model (STEAM3).

The Northern Sea Route (NSR) – a shipping lane stretching through Russian territorial waters from the Bering Strait in the East, along the Siberian coast, to the coast of Murmansk in the Barnet Sea – is the Arctic route with the highest navigation potential due to earlier and faster sea ice melting along the Russian coast (Melia, Haines, & Hawkins, 2016). The Arctic sea ice cover varies over the year and is observed at its minimum in September (Pierre & Olivier, 2015). However, considerable uncertainty is associated with the Arctic Sea ice extent. In 2020 a Siberian heat wave caused an average temperature of 10℃ above the summer normal in the region. The World Meteorological Organization (WMO) predicts a possibility of greater extremes in the future (WMO, 2021). Previous literature comparing the NSR with the Suez Canal Route (SCR) is dominated by empirical economic cost-benefit analyses (Theocharis, Pettit, Rodrigues, & Haider, 2018). Some of these studies have included emission estimates (H. Lindstad et al. (2016); Pierre and Olivier (2015); Schröder, Reimer, and Jochmann (2017); Schøyen and Bråthen (2011); Xu and Yang (2020); Zhao and Hu (2016), however only few studies have assessed exhaust emissions

other than CO_2 (H. Lindstad et al., 2016; Schröder et al., 2017). Schröder et al. (2017) compute exhaust emissions of CO2, NOx, and SOx given technical ship data input and ice condition input. Nevertheless, the climate impact of the emissions in terms of radiative forcing is not discussed. Furthermore, none of the studies comparing the NSR and the SCR have based their analysis on historical AIS data. H. Lindstad et al. (2016) calculate the climate impact of short-lived and long-lived emission species as a function of vessel design and power, though not using AIS data despite this data being available for the case vessel type.

1.2.3 Emission reduction tools

Shipping emissions depend on marine fuel and its content (Faber et al., 2020; Xu & Yang, 2020). Heavy fuel oil (HFO) is the lowest priced (DNV, 2019) and most widely used fuel in Arctic shipping (57% of fuel used and 76% of fuel carried) (Comer, 2019) and has a high content of sulfur and carbon (DNV, 2019; Faber et al., 2020). The IMO will implement a ban on using and carrying HFO in Arctic waters from 2024 due to adverse effects of potential oil spills in the region and to reduce impact of black carbon (IMO, 2020). A lighter fuel often used in the vessel's auxiliary engine is marine diesel oil (MDO) which has a sulfur content that complies to the IMO sulfur cap within environmental control areas (ECA) (Faber et al., 2020). Liquified natural gas (LNG), which mainly consists of methane and has a low sulfur and nitrate content (Pavlenko, Comer, Zhou, Clark, & Rutherford, 2020) is currently dominating the alternative marine fuel segment (DNV, 2021). LNG is typically burnt in dual-fuel engines, in which there are two distinct types. The *high-pressure* duel-fuel engine result in low methane slip, while *low-pressure* dual engines risk methane slip because of incomplete combustion, although lower emissions of NO_x (E. Lindstad, Eskeland, Rialland, & Valland, 2020).

The speed of a vessel depends on the vessels effective power. Reduced vessel speed, known as "slow steaming," has proven to be an effective operational strategy for fuel saving and emission reduction (Armstrong, 2013; Maloni, Paul, & Gligor, 2013; Tezdogan et al., 2016). The optimum speed for environmental performance is the speed that reaches the minimum SFOC, usually in the range of 65-80% engine load of maximum horsepower, depending on the engine. Operations at a lower or higher range increase the SFOC in grams of fuel per horsepower per hour (g/kWh) exponentially (Faber et al., 2020; Pastra, Zachariadis, & Alifragkis, 2021). Activity-based emission models can simulate the engine load and SFOC at different operational speeds. The maximum speed of a container vessel is generally between 23 and 25 knots, and slow steaming is

defined as 20-22 knots, extra slow steaming is between 17 to 19 knots, and super slow steaming is defined as 15 knots (Maloni et al., 2013). Moreover, the elasticity of speed reduction and emissions suggest that slow steaming is most efficient within the speed range of 25-14 knots. Below 14 knots, the CO2 elasticity becomes marginal, and slow steaming as a mitigation tool becomes less effective (Woo & Moon, 2014).

The current literature on Arctic shipping mainly comprises cost assessments related to navigability and projections of future sea ice extent. The few studies that include emission assessments focus on CO2 emissions and are, to a low extent, considering short-lived climate forcers and their local effect on the climate. More literature comparing the climate impact of the Suez Canal transit and Arctic transit is necessary to evaluate the feasibility of Arctic shipping in terms of environmental aspects. Fuel-saving strategies are discussed in the literature but are not often coupled with activity-based emission models. More activity-based tank-to-wake assessments should be done to either validate or contradict previous results and should be coupled with climate impact assessments of regional-specific emissions.

1.3 Research objective and report structure

Accessible Arctic routes give shorter distances and may lead to shorter travel time between Northeast Asia and Northern Europe leading to lower emissions and relieving the highly trafficked Suez Canal. There is a need for activity-based assessments of ship emissions that consider the climate impacts of different emission species relative to a reference gas to evaluate if re-routing vessels through the Arctic is a viable climate change mitigation strategy. The state-of-the-art ship emission assessment model called the MariTEAM model is used to investigate this. The objective of this master's thesis is to expand the MariTEAM model to include a re-routing feature that enables comparisons of original and new trade routes. Further, the extended model aims to demonstrate the application of the MariTEAM model as a tool to investigate the climate change impacts of re-routing container vessels through the Arctic based on vessel-specific emission calculations. The following research questions are used to examine this:

Main research question:

Does the re-routing from the Suez Canal Route (SCR) to the Northern Sea Route (NSR) offer climate change mitigation potential, and what are the related trade-offs?

Sub-questions:

- How can this be simulated using a state-of-the-art method?

- What are the implications and insights of applying different climate metrics?
- How do the insights from a current-generation model compare to those from previous generation models and their results?

This chapter has introduced the topic of maritime shipping globally and in the Arctic, the implications of different emission species, and previous studies using activity-based emission models. This knowledge serves as a foundation to answer the research questions. Following this introduction, chapter 2 is the method chapter, which introduces the MariTEAM model, its input data, and the climate metrics used in the analyses of the results. Further, chapter 3 presents a case study of five container vessels sailing from Shanghai in China to Rotterdam in the Netherlands and the implementation of the re-routing feature in the MariTEAM model. The case study includes a dual simulation where the baseline is the vessels running on HFO on the SCR. The baseline is compared to two experiments on a simulated Arctic route where the same ships sail on the NSR with (1) constant average speed and (2) constant voyage time as the baseline. The simulations are also run with MDO and LNG as alternative fuels to HFO. The results from the computations are presented in chapter 4 and discussed in chapter 5.

2 Methodology

To mitigate ship emissions, one must be able to quantify the emissions associated with shipping activities. This chapter presents the method used to quantify direct emissions from ship operations, so-called tank-to-wake emissions. An overview of the main characteristics, functionality, and data flows in the MariTEAM model is provided. Extensive model documentation is provided in Kramel et al. (2021). Please consult that source for more in-depth information, if desired. Further, this chapter presents metrics for a climate impact assessment used to normalize the climate impact of emissions.

2.1 MariTEAM model framework

The MariTEAM model (**Mari**time **T**ransport **E**nvironmental **A**ssessment **M**odel), developed by the Industrial Ecology Programme at NTNU (n.d,), calculates tank-to-wake ship emissions based on fuel consumption using a full bottom-up approach. Fuel consumption and emissions are simulated for a specific ship given the stated operational profile, information about ship location and weather conditions, and the specified fuel (HFO, MDO, or LNG). Figure 1 illustrates the model system from data sources to the final output of geo-specific emissions of carbon dioxide

(CO_2), methane (CH_4), nitrous oxide (N_2O), non-methane volatile organic compound (NMVOC), sulfur dioxide (SO_2), sulfate (SO_4), organic carbon (OC), carbon monoxide (CO), Elemental carbon (EC), and black carbon (BC). The three model inputs, the Automatic Identification System (AIS), the technical ship data, and the weather data, are combined to assess the required power output of the individual ships. The required power output of a vessel's engine is calculated separately for the main and auxiliary engine, and the instantaneous fuel consumption and exhaust emissions are computed by the technical details of the vessel's engine, the engine load, the type of fuel and its pollutant content (Johansson et al., 2017). The following sections explain the model input data and the emission calculations in the model.

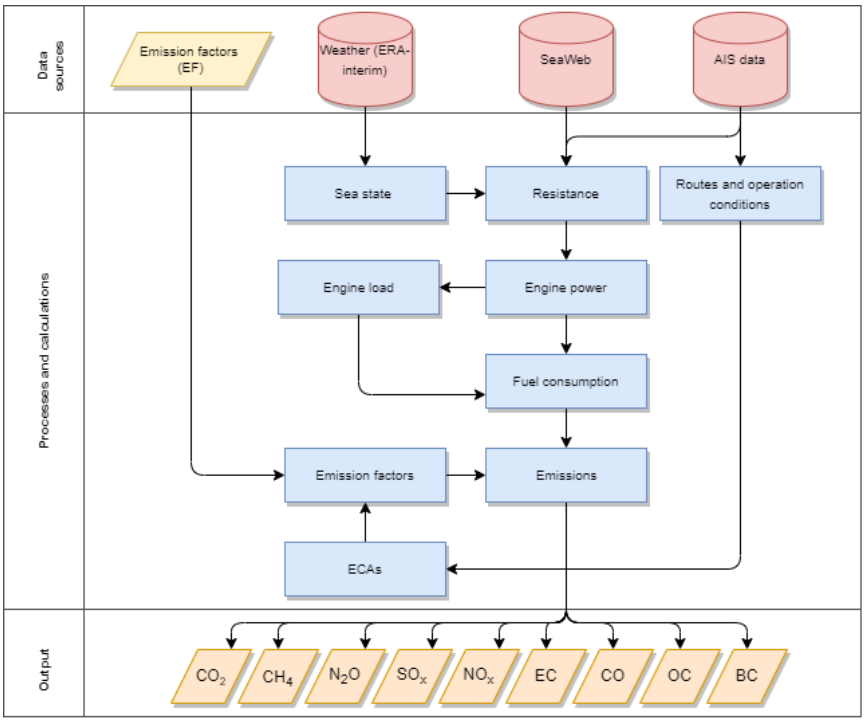

Figure 1. System illustration of the MariTEAM model. Emissions are computed based on fuel consumption, which is estimated from engine power given the sea state, resistance, and technical ship data on a given route. The illustration is based on Kramel et al. (2021).

2.1.1 AIS data

The Automatic Identification System (AIS) data reports actual vessel position with a few second intervals, including information about longitude and latitude points, heading, course, Unix timestamp, speed, and emission control areas (ECAs) (Johansson et al., 2017; Tichavska & Tovar, 2015). These elements make up the operational profile of an individual ship, including the change in distance (Δd_k) and time (Δt_k) from one timestamp to the next. In the MariTEAM model, the

AIS data is supplemented by data from the Norwegian Coastal Administration and the Norwegian Space Centre (NSC). Further, port calls from IHS Markit obtaining information about arrival and departure time from ports provide reference points to find the most likely shipping routes when missing data must be filled (Kramel et al., 2021). Suppose vessels running on HFO simulated in the model are located within an ECA. In that case, the engine operation switches to MDO, which has a sulfur content in compliance with the IMO regulations. For areas where the AIS data is scarce, especially in deep-sea regions, the model completes the route using an algorithm for interpolation. A demonstration of this feature is illustrated in Figure 2, adopted from Kramel et al. (2021).

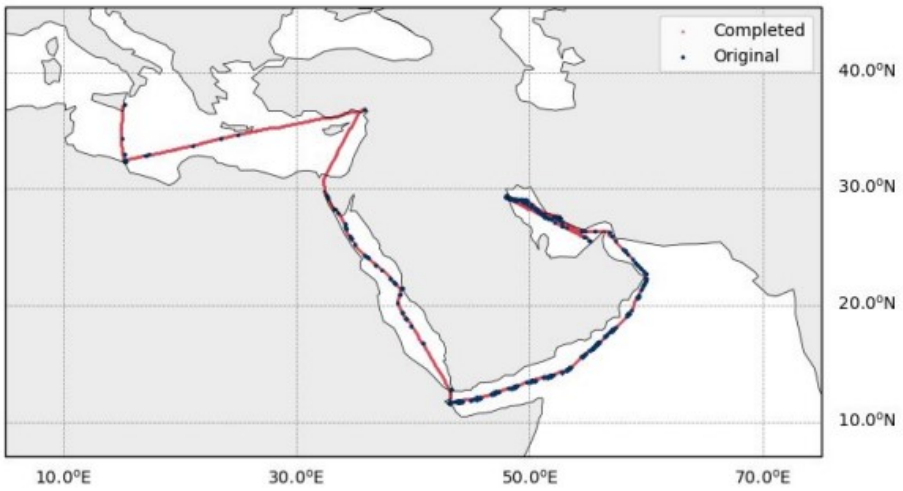

Figure 2. Demonstration of the algorithm used in the MariTEAM model to interpolate points in areas where AIS data is scarce. The illustration is adapted from Kramel et al. (2021).

2.1.2 SeaWeb

Technical ship data is the second input data in the MariTEAM model, allowing ship-specific emissions calculations based on engine type and ship design. The data is provided by the online ship register SeaWeb^{TM} provided by IHS Maritime & Trade. The database contains wide-ranging information about more than 200,000 IMO-registered vessels of 100 GT and above (IHS Maritime & Tarde, n.d.,). The elements from SeaWeb^{TM} included in the MariTEAM model are used to create the ship object and are listed below:

- MMSI number and ship type
- Construction year
- Deadweight tonnage (DWT)

- Light displacement tonnage (LDT)
- Breath, length, drought, and length between perpendiculars (length bp)
- Rated power, rotational speed (rpm), stroke, and engine cylinders of main engine
- Rated power of the auxiliary engine
- TEU (Twenty-foot equivalent unit)
- Number of reefer points (refrigerated containers)

2.1.3 Weather

The MariTEAM model simulation can be run with a basic module without weather data or with the weather module. Weather conditions at sea influence fuel consumption. If the resistance from waves and wind increases, the power output per distance sailed also increases as the ship must increase its engine power to maintain the same speed over ground (SOG) (Tezdogan et al., 2016). Considering these environmental factors could increase the global annual fuel consumption estimates by 5-15 percent, according to Johansson et al. (2017), and is thus a significant input to the model. The weather module in the MariTEAM model uses weather data acquired from the ERA-interim database provided by the European Centre for Medium-Range Weather Forecasts (ECMWF, n.d.,). The weather parameters used in the model are mean wave direction and mean wave period, significant wave height, and wind speed.

Figure 3 illustrates an example of a weather parameter retrieved from ECMWF used to calculate weather in the MariTEAM model. The V and U wind component show the northward and eastward wind, respectively, with a vertical coordinate at 10-meter height (Mladek, 2019). The figure scale ranges from -20.0 to 20.0 meters per second. Thus, the negative range on the V component illustrates the southward wind, and the negative range on the U component illustrates the westward wind. The maps in Figure 3 are simulation plots of the 10-meter V and U wind components from *July 1st, 2017*, retrieved from the ERA5 database. Wind direction and speed influence the vessel's resistance, and headwind leads to larger resistance, and the vessel must use greater power to maintain the same speed as in tailwind (Tezdogan et al., 2016). The westward wind is beneficial for a vessel sailing from East to West.

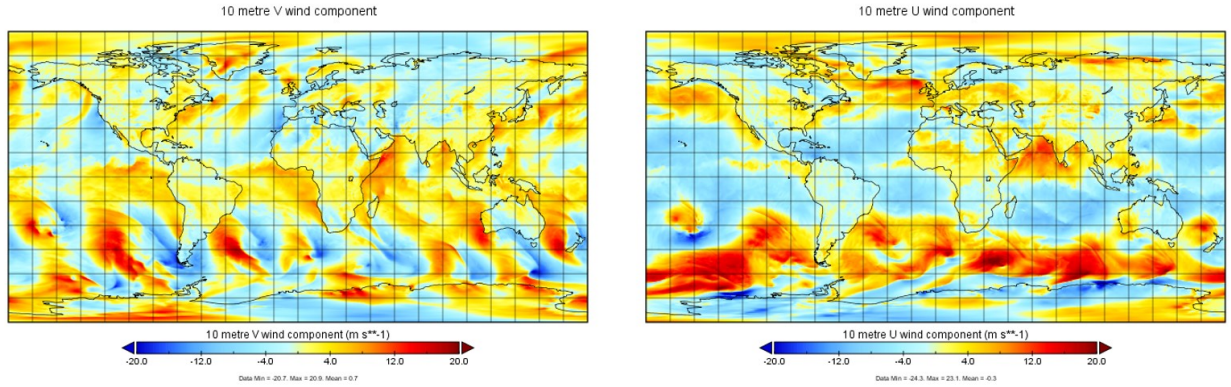

Figure 3. Illustration of the wind speed and direction, retrieved from the ECMWF ERA5 database. The data is used to calculate the weather at each AIS data point in the MariTEAM model. The V wind component shows the northward wind on the positive side of the scale and the southward wind on the negative side of the scale. The U component shows the eastward wind on the positive side of the scale and the westward wind on the negative side of the scale.

2.1.4 Estimation of ship emissions

CO_2 and SO_x emissions from engine combustion are highly dependent on fuel consumption, as they depend on the pollutant content in the fuel. These emissions are thus calculated by multiplying the power output (P_S) by the fuel consumption and the fuel-based emission factor (FC), i.e., the content of the emission species in the given fuel of each vessel (Kramel et al., 2021), as illustrated in equation (1).

$$E_{i,j,k} = \sum P_{S_{j,k}} * SFOC_{i,j} * FC_{j,k} * \Delta t_k \quad (1)$$

The fuel consumption in the MariTEAM model is calculated based on engine load and specific fuel oil consumption ($SFOC$). The engine load determines the engine's combustion efficiency, which affects the composition of pollutants (Jalkanen et al., 2012). An engine's load factor (LF) is the actual power output relative to the maximum continuous rated power output (MCR). SFOC is the measured mass of fuel consumed per unit time per kW, which is assumed to vary as a function of the engine load (Ananth, 2021). At very low or very high loads, the SFOC tends to be high (Faber et al., 2020). Sulfur content in the MariTEAM model is approximated to 2.6% in mass for HFO and 0.08% for MDO and LNG, as in compliance with the 2012 IMO sulfur cap. The sulfur oxides are split into SO_2 and SO_4 by 97% and 3%, respectively (Kramel et al., 2021).

Other emissions occur due to incomplete combustion and are thus calculated differently than CO_2 and SO_x. Engine power output (P_S) is multiplied by energy-based emission factors (EF) given in gram pollutants per kWh (Faber et al., 2020). The energy-based emissions are corrected by engine load as a percentage of MCR (LF) (Kramel et al., 2021). The energy-based emission equation is illustrated in equation (2).

$$E_{i,j,k} = \sum P_{S_{j,k}} * EF_{i,j} * LF_{j,k} * \Delta t_k \quad (2)$$

The exceptions from this calculation method are NO_x emissions specified by the maximum allowance according to the IMO regulations and BC estimated by regression curves based on the study of several engines (Kramel et al., 2021). In the equations above, i is the pollutant of interest, j is the engine (main or auxiliary), and k is the route section. Δt_k is the change in time t in seconds between observation points on route k.

2.2 Climate impact metrics for exhaust emissions

The MariTEAM model simulates ship activity and computes the magnitude of emissions per emission species in kilograms, as illustrated in Figure 1. As explained in section 1.2.1, the different emission species have different radiative efficiencies and lifetimes in the atmosphere. The emissions need to be normalized on a common scale to assess the relative impact of the emissions in terms of climate change potential. This is done by multiplying the magnitude of a given emission by the corresponding metric value. The metric value depends on the time horizon and whether the metric is instantaneous or integrative (Gasser et al., 2017). Due to the short lifetime of SLCFs, the effect of these climate forcers on the global temperature is more evident on a short time horizon (e.g., 20 years) than CO_2, which affects the global temperatures after 100 years (Lund et al., 2020). A metric with a time horizon of one hundred years may thus partly exclude the climate impact of the short-lived species. Hence, the time horizon chosen for the climate metric will highly affect the impact assessment results (Peters, Aamaas, T. Lund, Solli, & Fuglestvedt, 2011).

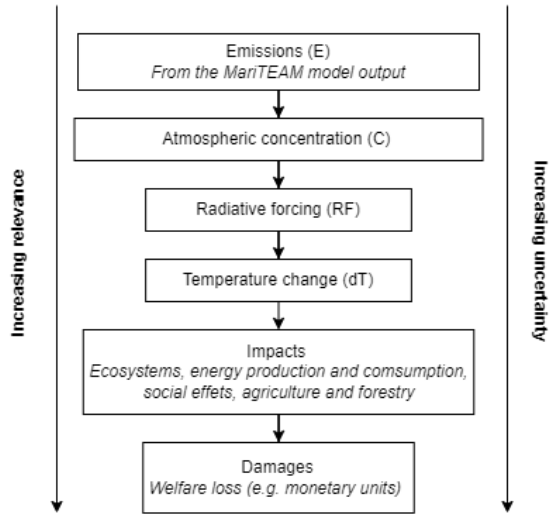

Figure 4. Cause-effect chain of potential climate effects of emissions (based on Fuglestvedt et al., 2003)

The choice of climate metric depends on the purpose of the measurement (Myhre et al., 2013b). Figure 4 illustrates the cause-and-effect chain for the potential climate effect of the emissions. The first parameter that allows for direct comparison of climate impacts from emissions is the radiative forcing, which is used to calculate the *Global Warming Potential (GWP).* The GWP is the integrated (cumulative) radiative forcing (RF) due to a pulse emission of a given species, *i*, over a time-horizon (TH) and relative to the pulse emission of CO_2 (Shine et al., 2005). The most widely used emission metric is the GWP over a TH of 100 years (GWP100), but to account for short-lived substances, one can use GWP over a TH of 20 years (GWP20). Despite its name, GWP does not represent the effect of pulse emissions on temperature. Two gasses with different lifetimes before atmospheric decay (e.g., CO_2 and CH_4) can cause different temperature responses at a given time due to the difference in strength (Shine et al., 2005).

Another metric called the G*lobal Temperature change Potential (GTP)* can be applied to represent the global-mean surface temperature change (Shine et al., 2005). This metric moves a step further down the cause-effect chain from radiative forcing and states the potential temperature change at a particular time in the future by combining the RF with the behavior of the temperature response of the climate system at time t (J. S. Fuglestvedt et al., 2010; Aamaas, Peters, & Fuglestvedt, 2012). With the GTP metric, as opposed to the GWP metric, a pule emission of 1 kg of a given gas, x, will give the identical temperature change in year t as $GTP^x(t)$ kilograms of the reference gas (carbon dioxide) (Shine et al., 2005).

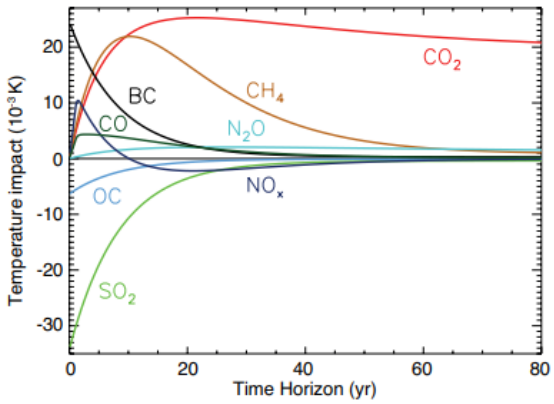

Figure 5. Temperature response by emission specie for the total anthropogenic emissions for a 1-year pulse. The x-axis shows the time horizon in years, and the y-axis shows the temperature response (adapted from Myhre et al. (2013b)).

Figure 5 illustrates the temperature impact of different emission species over time. CO_2 persists in the atmosphere for the longest time and contributes to significant warming. At GTP20, NO_x has reached its lowest temperature potential, while SO_2 has significantly decayed. As illustrated in Figure 4, the relevance for policymakers increases down the cause-effect chain as the impact of emissions can be tied to impacts on nature and society and damage and welfare loss. Simultaneously, each step of the cause-effect chain is associated with increased uncertainty, as it requires additional assumptions (Shine et al., 2005).

Metric values for GWP and GTP used in the climate impact assessment in this report are retrieved from IPCC 5th Assessment report (Myhre et al., 2013a) and listed in Table 1. CO_2, CH_4, N_2O, OC, and CO are given as global mean values, while NO_x and SO_2 metric values are shipping-sector specific. In addition, for GWP, the sector-specific metrics include Arctic-specific values for SO_2, BC, and OC. The shipping- and Arctic-specific GWP metric for BC includes the impact of soot deposited on snow in addition to soot emitted to air. All Arctic metric values are provided by Ødemark et al. (2012). The NO_x and SO_2 metric values used for calculating the climate impact of shipping in this report are the values provided by J. Fuglestvedt, Berntsen, Myhre, Rypdal, and Skeie (2008).

Table 1. Metric values for GWP and GTP of TH20 and TH100 adapted from the Supplementary Material in IPCC 5th Assessment Report (Myhre et al., 2013a).

Global-mean metric values				
Emission species	GWP20	GWP100	GTP20	GTP100
CO_2	1	1	1	1
CH_4	83.4	28.5	67.5	4.3
N_2O	263.7	264.8	276.9	234.2
BC	2421.1	658.6	702.8	90.7
OC	-244.1	-66.4	-70.9	-9.1
CO	5.9	1.9	3.7	0.3
Shipping sector-specific metric values				
NO_x[a]	-31	-25	-160	-4.2
SO_2[a]	-150	-43	-44	-6.1
SO_2, Arctic[b]	-47	-13	-	-
BC, Arctic[b]	2801	796	-	-
OC, Arctic[b]	-151	-43	-	-

[a] J. Fuglestvedt et al. (2008)

[b] Ødemark et al. (2012)

3 Case study: Rerouting container vessels through the NSR

The objective of this master's thesis is to assess the MariTEAM model as a simulation tool to reroute vessels through the Arctic as an alternative route to the conventional Suez Canal route between East Asia and Western Europe. The aim is to compute the potential emissions to air associated with Trans-Arctic shipping and compare the climate impact of exhaust emissions on the two routes. This chapter presents the case study of five container vessels, and the implementation procedure of the model expansion to account for the rerouting is explained. The chapter is divided into three sections: firstly, a section explaining the modifications done to the vessels' operational profiles; secondly, a section describing the experiment design and assumptions; and thirdly, a section explaining the implementation of a new Arctic route simulation in the MariTEAM model.

The case study simulates a one-way voyage from the Yangshan Deep Water Port in Shanghai to the Maasvlakte Port in Rotterdam. Figure 6 illustrates a map of the two routes assessed in the simulations. The blue line is the SCR, which is simulated based on the AIS data input in the MariTEAM model, while the orange line is the NSR lane computed manually. The NSR has different shipping lanes that vary in distance from the Siberian coastline. The Arctic route simulated in this case study follows what Schröder et al. (2017) defined as an intermediate route

because the sea ice is thinner and retreats earlier close to the coast (Aksenov et al., 2017; Melia et al., 2016).

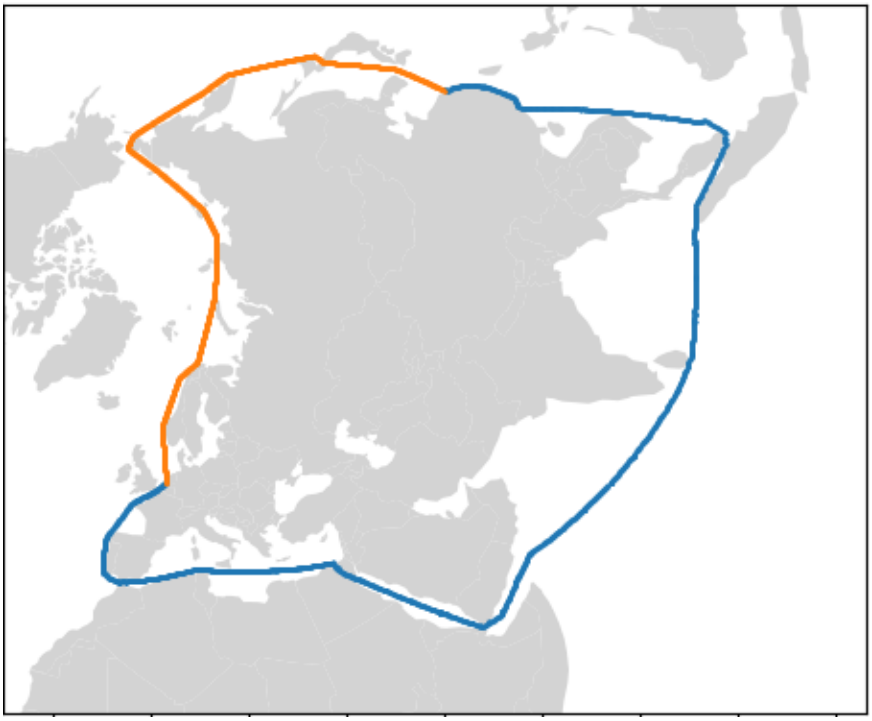

Figure 6. Map of the SCR (blue line) and NSR (orange line) simulated in the MariTEAM model. The Arctic route simulated in this report is close to the coast because of the uncertainty concerning ice thickness and extent further north. The ice retreats earlier along the coast.

3.1 The modified operational profiles

Container ships are one of the vessel types most frequently transiting the Suez Canal and are essential for Eurasian trade (Zheng et al., 2018). Therefore, container vessels were the sub-section of vessels chosen for this case study. Five container vessels from the Danish international container shipping company Maersk Line (Maersk, n.d.,) were selected for the case study. The container vessels were obtained from Maersk's own schedule website and paired with the SeaWeb^{TM} technical ship data in 2017. AIS data, weather data, and the technical ship data compute the operational profiles (OPs) of the five vessels and are thus the baseline OPs for the case study. The technical ship data from SeaWeb^{TM} for each vessel is listed in Table 2. All the selected vessels sail back and forth between Shanghai and Rotterdam throughout the entire year and include port calls in countries such as Singapore, Korea, Malaysia, England, and Denmark. The operational profiles in the MariTEAM model includes variables such as longitude and latitude of location, the time of

location (Unix timestamp), the change in distance, Δd_k and time, Δt_k between each location, whether the vessel is located within an Environmental Control Area (ECA), the speed over ground (SOG) at each location point, and weather variables such as wave hight and wind speed.

Table 2. Technical ship data for the case vessles retrieved from SeaWeb™.

Technical ship data	*Magleby*	*Mary*	*Madison*	*Marstal*	*Majestic*
MMSI	219018986	219018692	219018864	209019139	219018501
Built (year)	2014	2014	2013	2014	2013
Breadth (m)	59.0	59.0	59.0	59.0	59.0
Draught	16.0	16.0	16.0	16.0	16.0
Length (m)	399.2	399.0	399.2	399.2	399.0
Length bp (m)	376.21	376.21	376.21	376.21	376.21
DWT	194417.0	194252.0	194394.0	194692.0	194431.0
LDT	54583.0	54748.0	54606.0	54308.0	54569.0
ME rated power (kW)	59360.0	59360.0	59360.0	59360.0	59360.0
ME rpm	73.0	73.0	73.0	73.0	73.0
ME stroke	2	2	2	2	2
ME cylinders	8.0	8.0	8.0	8.0	8.0
AE rated power (kW)	3880.96010	3880.96010	3880.96010	3880.96010	3880.96010
Service speed (knot)	19.0	19.0	19.0	19.0	19.0
TEU	18340	18340	18340	18340	18340

The baseline OPs were modified to simulate a one-way voyage from Yangshan Port in Shanghai to Maasvlakte Port in Rotterdam with no other port calls during the summer season of 2017. The flowchart in Figure 7 illustrates the code that was implemented to filter the individual OPs. The operational profiles were filtered to delete all data points representing activity before the port call in Shanghai and after the port call in Rotterdam. The OPs were then adjusted to exclude all port calls on the route by deleting all rows with SOG = 0. The timestamp was adjusted as a function of the distance between each coordinate point (Δd_k) and the operational SOG to match the Unix timestamps with the modified OPs. The final output of this code is a baseline operational profile for each of the five container vessels sailing on the SCR. The Python code can be found in *Appendix A.1*.

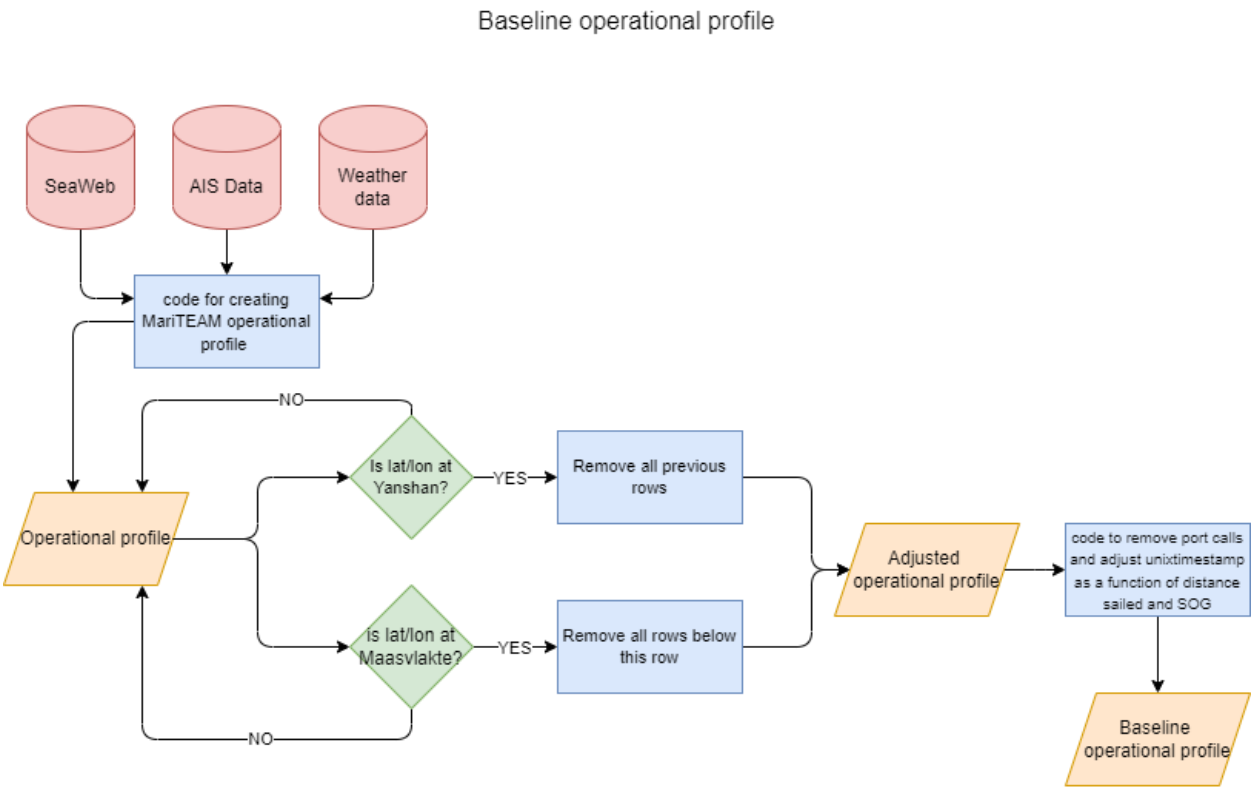

Figure 7.Flowchart of baseline operational profile code. The operational profile of each ship is modified to account for a one-way voyage from Yangshan Port in Shanghai to Maasvlakte Port in Rotterdam. The Python code can be found in Appendix A.1.

3.2 Experiment design and assumptions

The experiments simulated through the MariTEAM model in this thesis aim to depict the difference in emissions associated with the two alternative trade routes. The implementation of the alternative Arctic route is explained in detail in section 3.3, but first, this section describes the experiments conducted based on the baseline OPs and the Arctic OPs. In addition, the assumptions considered in this study are provided.

Table 3 lists the experiments conducted in this thesis. Two experiments are conducted and compared to the baseline operational profile through model expansion. The experiments are designed as dual simulation experiments where the baseline OPs are compared to the new Arctic OPs of the respective vessels with one variable (speed or voyage time) held constant. In the first experiment, the speed of each vessel on the Arctic route is set equal to the average speed of the original vessel activity in the baseline OPs. This experiment is denoted *Cv.* The engine combustion emissions highly depend on the vessels' speed over ground (SOG) (Faber et al., 2020; Xu & Yang, 2020). When SOG is equal to the average speed of the baseline, one can analyze the net difference

in climate impact resulting from the difference in travel duration between the two routes. In the second experiment, the voyage time on the Trans-Arctic route is set equal to the voyage time of the SCR. This experiment is denoted *Ct*. As the distance in nautical miles is shorter between Yangshan Port and Maasvlakte Port on the NSR, this allows for slower operational speed in the Arctic OP than the baseline. As suggested in the literature (Armstrong, 2013; Maloni et al., 2013; Tezdogan et al., 2016), slow steaming is an operational measure that can lead to less fuel consumption and thus lower emissions, and the effect of slow steaming on emissions are therefore tested in the second experiment.

Based on the technical ship data from SeaWeb^{TM}, the vessels are assigned HFO as fuel in the main engine and MDO as fuel in the auxiliary engine in the MariTEAM model. When the vessels are outside of an Environmental Control Area (ECA), they run on HFO. Within the ECAs, the vessel switches to MDO to meet the international regulations on sulfur emissions. The routes are, in addition, simulated with alternative fuels as a second layer to the experiments. The HFO-ban in the Arctic region will take effect in 2024 (IMO, 2020). The potential effects of an HFO-ban are assessed in a third simulation of the vessels run exclusively on MDO on the NSR. In addition, a fourth experiment is conducted by simulating both routes sailed with LNG as fuel in the main and auxiliary engines to investigate a scenario where low-carbon fuels are dominating the shipping sector.

Table 3. List of experiments conducted in the thesis. Experiment 1 and 2 are conducted through model expansion, while experiment 3 and 4 is conducted by changing the fuel mix in the MariTEAM model.

Experiment list
Baseline operational profiles compared to Arctic operational profiles with:
1. Constant speed (*Cv*)
2. Constant voyage time (*Ct*)
3. HFO-ban in the Arctic (MDO as fuel on the Arctic route)
4. LNG as fuel on both routes

The following assumptions related to the navigability of the Arctic route and the research scope are proposed to make the dual simulation of the SCR and the NSR comparable:

1. The case vessels are designed for the SCR and are large due to the advantages of economies of scale (UNCTAD, 2020). The same vessel size is assumed for the simulation on the NSR, as the same technical profiles are applied for the Arctic simulation.
2. According to the Northern Sea Route Administration (NSRA), vessels without an ice class are allowed independent navigation along the NSR in ice-free water (NSRA, 2020). The literature suggests that the ice extent is the lowest in September (Melia et al., 2016; Pierre & Olivier, 2015). The MariTEAM model does not account for historical sea ice extent and thickness. The Arctic Sea is thus assumed to be ice-free in September 2017, which eliminates the need for ice-class or ice breakers.
3. The baseline and the Arctic voyages are assumed to have no port calls for transhipments or fuel refill along the routes.
4. The analysis does not consider capital expenses of potential redesign needed for Arctic navigation or to use alternative fuels. The experiments are based on the vessels having the same characteristics on the SCR and the NSR.
5. This study considers only the emissions to air and its climate impact. It does not consider any operational costs related to fuel consumption, container handling fees, or fees to transit the Suez Canal of the Russian-owned NSR.

3.3 Implementation of the Arctic route in the MariTEAM model

The simulated SCR is based on historical AIS data from 2017 that provides the time and location of the individual vessels. On the other hand, the coordinates were manually plotted for the implementation of an Arctic route, as no AIS data is available for the container vessels in the Arctic region. Thus, the coordinate data from the AIS database is replaced by manually plotted coordinates of a likely Trans-Arctic route, based on previous literature and activity data from MarineTraffic.com (MarineTraffic, n.d.,). The coordinates were found by identifying seventeen coordinate nodes on the route through the Sea of Japan (East Sea), the Bering Strait, the Siberian coast, the Norwegian Sea, and the North Sea. Further, a linear interpolation between the nodes computes latitude and longitude points with a consistent geospatial resolution for the whole route. The kilometer distance between each coordinate point was saved as a new Δd_k variable to calculate the change in time, Δt_k, between each coordinate. Unix timestamps were identified based on the first Unix timestamp of the baseline OPs to set the start time of the Arctic voyage equal to the Suez Canal voyage.

For experiment 1 (Cv) with constant average speed, the SOG of the vessels on the Arctic route is set equal to the average SOG of the original OPs. Further, the SOG was changed from the unit knots to the unit km/s. The Δd_k was then divided by the speed (km/s) to get a new output for the change in the time between each coordinate point, Δt_k. For experiment 2 (Ct) with constant voyage duration, the Δt_k for the baseline OPs were implemented as the change in the time between each coordinate point in the Arctic OPs. The SOG in the Arctic OPs were then derived by dividing the Δd_k by Δt_k. As for the first experiment, the Unix timestamp in the Ct experiment was found by adding the new Δt_k to the first Unix timestamp in the baseline OPs. Figure 8 illustrates the coding procedure as a flow chart. The actual codes are to be found in *Appendix A.2*. The weather data from the baseline OPs were replaced by weather data from the ERA5 database matching the location of the vessels on the Arctic route. From the database, historical weather of September 2017 data was imported. The technical ship data for each vessel was then run in the MariTEAM model with the new Arctic operational profile and weather profile.

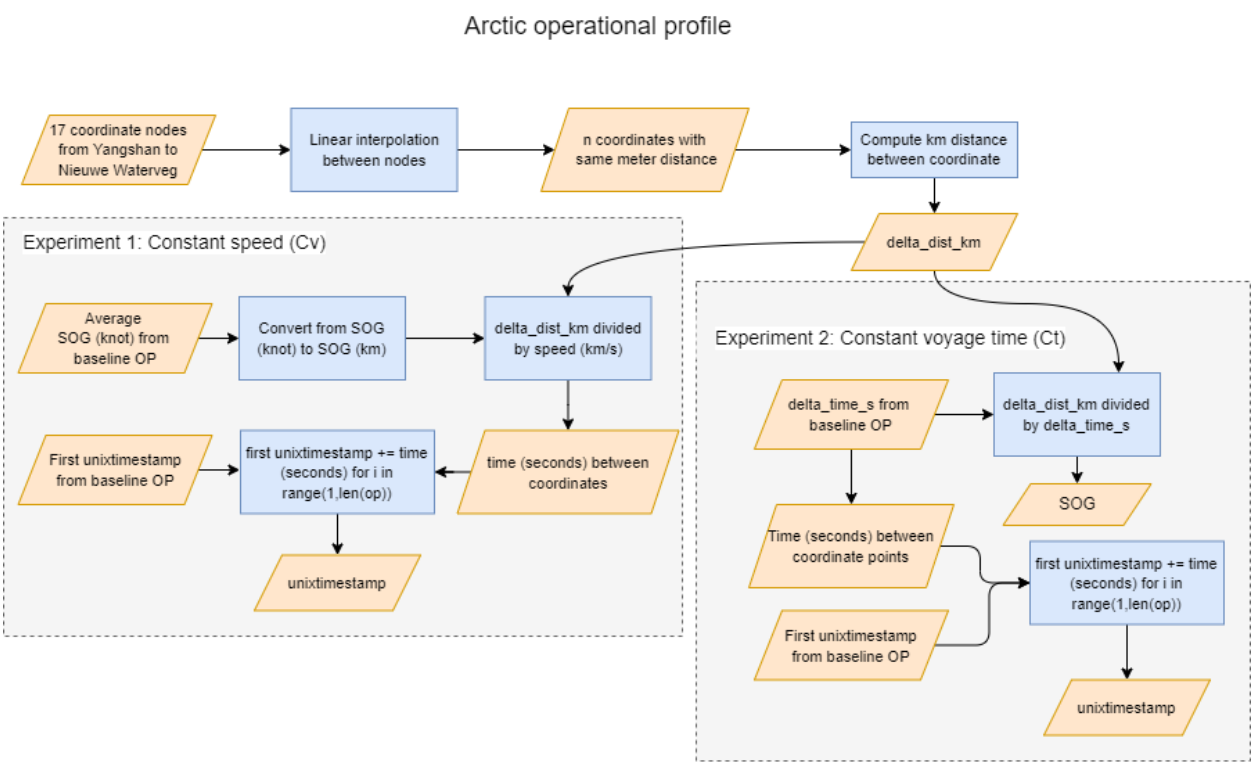

Figure 8. Flowchart of the coding procedure for the Arctic operational profiles. The flowchart shows the procedure for experiment 1 with constant average speed (Cv) and experiment 2 with constant voyage time (Ct). The Python code can be found in Appendix A.1

The case study, experiments, and model expansion procedure have been explained in this chapter. The output from the model simulation is the computation of fuel consumption, power output, weather state, and emissions associated with each coordinate point on the vessel routes. These results, in addition to the results from the climate impact assessment, are presented in the next chapter.

4 Results

This chapter presents the results from the model simulation of the five vessels on the SCR and the NSR. Firstly, simulation results on vessel operation are presented to visualize the functionality of the simulation model. Further, statistical results are presented to show the variation in vessel activity given the assumptions, and lastly, the calculated climate impact of each experiment is presented. The experiments on the NSR will, from here on, be designated Cv (constant average speed) and Ct (constant voyage time).

4.1 Descriptive results of vessel operation

The voyage time from Shanghai to Rotterdam depends on the navigational distance and the speed of the vessels. The distance in nautical miles and the percentage difference between the SCR and the NSR are presented in Table 4. On average, the NSR is 10% shorter than the SCR for all vessels; however, the actual route taken on the SCR varies, which means that the difference in distance sailed on the NSR versus the SCR varies from vessel to vessel.

Table 4. Table displaying the calculated distance between origin port and destination port in nautical miles with percentage difference in navigational distance between the SCR and the NSR.

Distance from Shanghai to Rotterdam in nautical miles						
	Marstal	*Majestic*	*Mary*	*Magleby*	*Madison*	*Average*
SCR	11095	11036	11218	10226	10835	10882
NSR	9806	9806	9806	9806	9806	9806
% Difference	12 %	11 %	13 %	4 %	9 %	10 %

Table 5 describes the speed range of the respective operational profiles. The average speed of each vessel on the SCR (baseline OPs) is the constant speed assigned to each vessel on the NSR in the Cv OPs. All baseline OPs have a median speed ranging from 19 to 20.1 knots, around the service speed of the vessels of nineteen knots. The average speed of the baseline vessels is equal to the

median speed for all vessels except for *Marstal*, which has an average speed of 0.7 knots slower than the median speed. *Madison* has the highest maximum speed (23.9 knots) and the highest minimum speed (14.4 knots). *Majestic* has the most extensive speed range, from a minimum of 2.0 knots to a maximum of 23.2. In the Ct OPs, the voyage time is equal to the voyage time in the baseline OPs, which allows for slow steaming with speed reduction ranging from 0.9-4.2 knots, depending on the voyage.

Table 5. The speed over ground (SOG) varies within the baseline operational profiles (OPs) and is obtained from AIS data. The mean speed of each baseline OP is the assigned constant speed of the case vessels in each Cv OP. The Ct experiment has a reduced constant speed to match the voyage duration of the baseline OPs.

Speed over ground for baseline OPs					
	Marstal	*Majestic*	*Mary*	*Magleby*	*Madison*
Max	21.3	23.2	22.6	21.4	23.9
Min	1.5	2.0	2.5	8.3	14.4
Median	19.9	19.5	20.1	19.0	19.6
Mean (Cv SOG)	19.2	19.5	20.1	19.0	19.6
Ct SOG	16.2	15.3	16.0	18.1	17.6

Table 6. The table displays the number of days, hours, and minutes each vessel spends on the respective routes. The baseline is the SCR, and Cv and Ct are the Arctic route with different speeds. In the Ct experiment, the voyage duration equals the voyage duration of the baseline. Cv has a reduced voyage time ranging from one to four and a half days.

Voyage duration per vessel and experiment			
	Baseline	*Ct*	*Cv*
Marstal	25 days, 6 hours, 46 min	25 days, 6 hours, 46 min	21 days, 7 hours, 1 min
Majestic	26 days, 15 hours, 26 min	26 days, 15 hours, 26 min	22 days, 0 hours, 47 min
Mary	25 days, 12 hours, 13 min	25 days, 12 hours, 13 min	21 days, 3 hours, 19 min
Magleby	22 days, 14 hours, 32 min	22 days, 14 hours, 32 min	21 days, 12 hours, 52 min
Madison	23 days, 5 hours, 9 min	23 days, 5 hours, 9 min	21 days, 2 hours, 17 min

Table 6 displays the voyage duration per vessel and experiment. The Ct experiments have the same voyage duration as the Baseline, and the Cv experiments have a shorter voyage duration. *Magleby* has the lowest reduction in voyage duration in experiment Cv, while *Majestic* has the most considerable reduction in voyage duration.

Figure 9 presents the relationship between specific fuel oil consumption (SFOC) and the main engine load for the baseline vessels. The lowest SFOC for the baseline OPs is 170 g/kWh at a load of around 75%. At low loads (below 45%), the SFOC exponentially increases towards the maximum of 254.36 g/kWh. This high SFOC is observed for all the vessels except *Madison.* For

the experiments on the NSR with constant average speed (Cv) and constant voyage time (Ct), all vessels have marginal variations in engine load and SFOC.

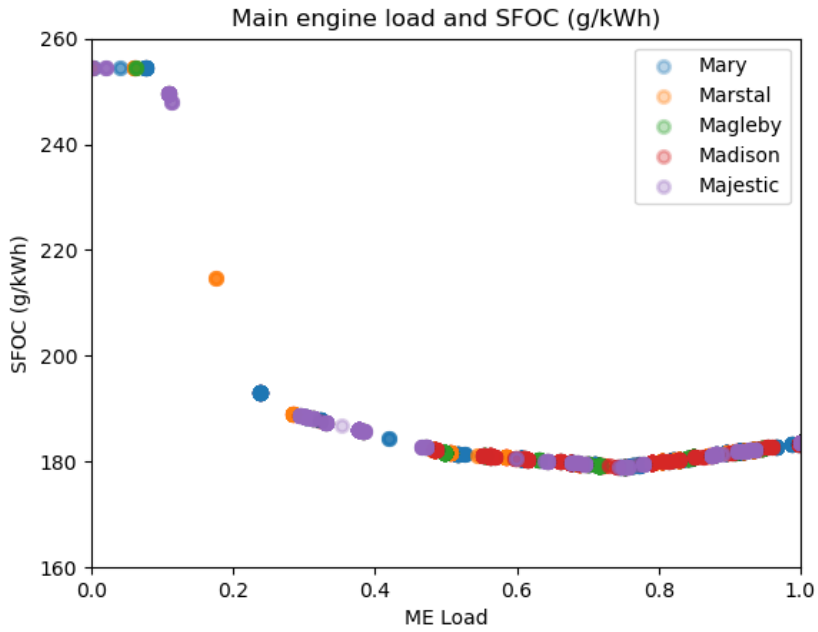

Figure 9. The relationship between specific fuel oil consumption (g/kWh) and min engine load in the baseline OPs. The colored scatter plots represent each case vessel.

Table 7 lists the median values for load and SFOC in all three experiments. The variation in load and fuel oil consumption between the vessels is the largest for the Ct experiment, where *Magleby* has the lowest constant SFOC of 180.46 g/kWh at 61% load, and *Majestic* has the highest of 185.63 g/kWh at 39% load. However, the overall lowest SFOCs are observed in Cv, where the fuel consumption ranges from 179.13 to 179.89 g/kWh at loads ranging between 67-76%. The lowest SFOC observed in Cv is the one of *Magleby* (180.46 g/kWh), which runs on a load of 71%. The other vessels with both lower and higher loads than this have a higher SFOC.

Table 7. The median SFOC(g/kWh) and ME load (%) for each case vessel and simulation experiment.

Median SFOC (g/kWh) and ME load (%)						
	Baseline		**Cv**		**Ct**	
	SFOC	*ME Load*	*SFOC*	*ME load*	*SFOC*	*ME load*
Marstal	181.8	83 %	179.2	74 %	183.6	44 %
Madison	180.6	79 %	179.1	76 %	181.0	57 %
Magleby	179.4	72 %	179.4	71 %	180.5	61 %
Mary	181.9	85 %	179.1	76 %	183.9	43 %
Majestic	183.5	77 %	179.9	67 %	185.6	39 %

Main engine fuel consumption in the baseline OPs increases with speed and engine power output, as displayed in Figure 10. The graphs show the fuel consumption of the main engine in kilograms per nautical miles on the y-axis and the speed over ground (knots) and the main engine power output (kW), respectively, on the x-axes. The graph shows a peak fuel consumption (approximately 150 kg/nm) at 21 knots. The ME rated power of the vessels is 59 360 kW (Table 2), and the graph shows that the highest fuel consumption occurs at this rated power. Most of the observed speed on the SCR is between 16 and 21 knots, and the engine power is most frequently observed to be above 30 000 kW.

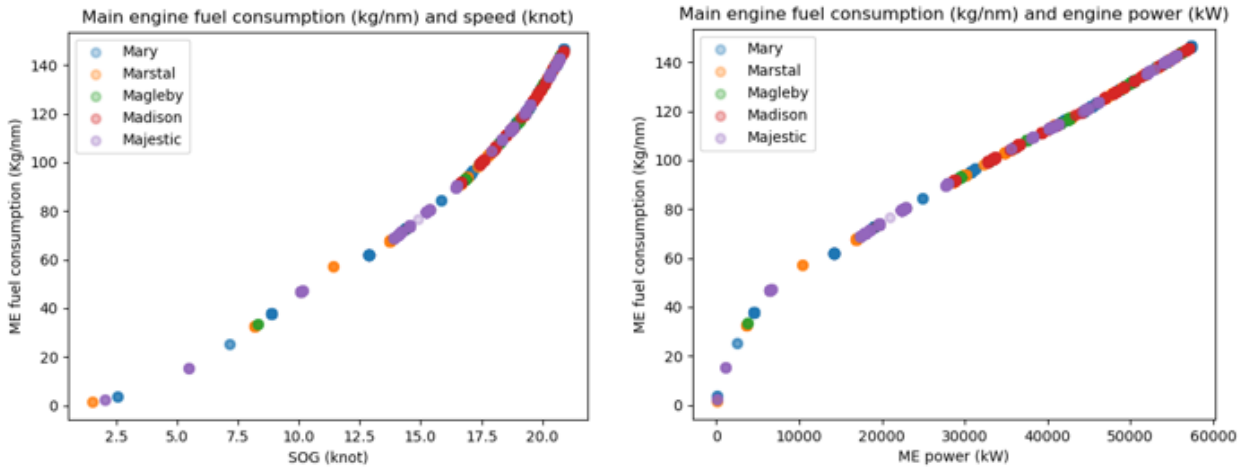

Figure 10. The relationship between speed (knot) and fuel consumption (kg/nm) to the left and main engine power(kW) and fuel consumption (kg/nm) to the right. Fuel consumption increase with SOG and ME (Main Engine) power in the Baseline OPs.

4.2 Weather impact on fuel consumption

The two figures below show the significant wave height and wind speed on the routes for the case container vessel *Mary*. The time on the x-axis is based on the Unix timestamps of the operational profiles, which is the same for all routes because the Arctic OPs are built up based on the start time and arrival time of the baseline OPs. The y-axes show the wave height in meters (Figure 11) and wind speed in meters per second (Figure 12). The baseline OPs are assigned weather data from the ERA-interim database that correspond to the time and vessel location from the AIS data. The Arctic OPs (Cv and Ct) have been assigned weather data from the ERA5 database. Historical weather data from September 21st, 2017, is assigned to each longitude and latitude point in the Arctic operational profiles. The weather representation on the Arctic route is thus based on a one-day weather observation at a time of the year when the sea ice is assumed to have retreated from

the coastline. Cv and Ct have the same weather pattern; however, Ct is lagging because of the slower speed that makes the vessels reach the specific locations later than the vessels in the Cv experiment.

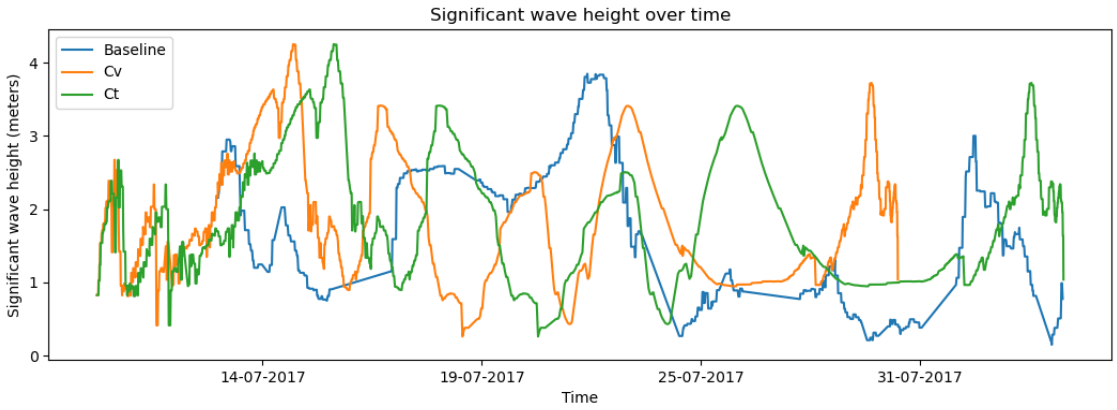

Figure 11. Significant wave height in meters over time for the three operational profiles of the container vessel "Mary."

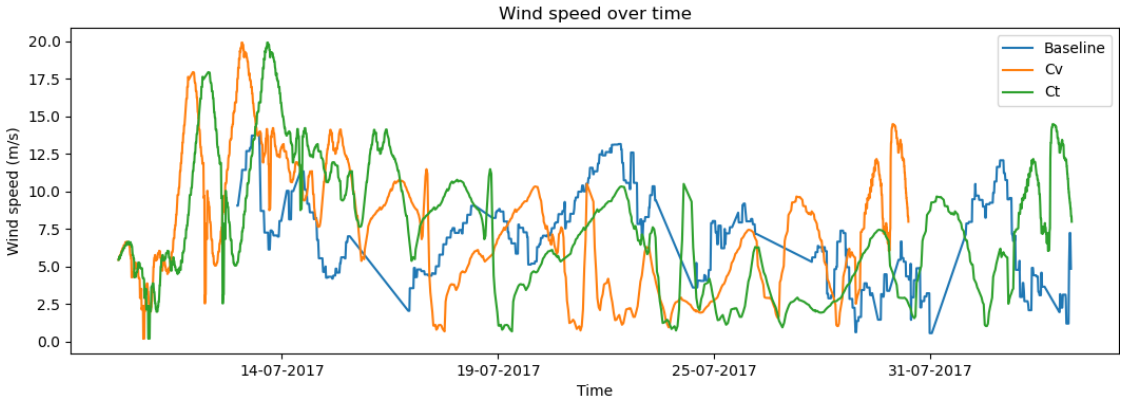

Figure 12. Wind speed in meters per second over time for the three operational profiles of the container vessel "Mary."

The wind speed time series does not display the direction the wind is going; however, it portrays the degree of wind in terms of speed (m/s). The significant wave height and wind speed have higher average values for the Arctic OPs than the baseline OPs.

To illustrate the weather effect in the MaritTEAM model, the Cv OPs were run with and without the weather module to investigate the fuel consumption associated with the Arctic route in calm weather and with the weather data from September 2017. Table 8 shows the kilograms of fuel consumed per nautical miles in the Cv OPs with and without weather data applied. The results show that the weather effect accounts for ~8% of the kg of fuel consumed per nautical mile.

Table 8. Fuel consumption (kg) per nautical mile is assessed for the Cv OPs with and without the weather module. The fuel consumption (kg/nm) and the percentage difference between simulation with and without weather are listed for each case vessel.

Fuel consumption (kg/nm) for Cv OPs run with and without weather data				
	With weather	W/o weather	difference in kg/nm	% difference
Marstal	408	378	30	7.8 %
Madison	416	385	31	8.0 %
Magleby	399	370	29	7.8 %
Mary	416	386	30	7.8 %
Majestic	384	356	28	7.9 %

4.3 Operational fuel consumption variations and emission results

Presented in Table 9 is the total fuel consumed in tons per voyage for each vessel in each experiment with weather input data, including the percentage decrease in fuel consumption in Cv and Ct compared to the baseline. The average fuel consumption of the baseline OPs is 4467 tons per voyage. The fuel consumption is reduced by 11.2% and 30.6% on average for the Cv and Ct OPs, respectively.

Table 9. Tons of fuel consumed per voyage for each vessel and experiment. The table also displays the percentage change in fuel consumption relative to the baseline OPs and the change from Cv to Ct.

Fuel consumption tons/voyage						
	Baseline	*Cv*	*% Change from baseline*	*Ct*	*% Change from baseline*	*% Change from Cv*
Marstal	4553	3999	-12.2 %	2933	-35.6 %	-26.7 %
Madison	4632	4078	-12.0 %	3394	-26.7 %	-16.8 %
Magleby	4395	3912	-11.0 %	3566	-18.9 %	-8.8 %
Mary	4553	4084	-10.3 %	2906	-36.2 %	-28.8 %
Majestic	4204	3764	-10.5 %	2713	-35.5 %	-27.9 %
Average	4467	3967	-11.2 %	3102	-30.6 %	-21.8 %

Figure 13 displays a box and whiskers plot of the variation of fuel consumption within the different baseline operational profiles. Although the case vessels have similar technical profiles, the routes vary in navigational distance. Therefore, the fuel consumption is divided by transport work (DWT-nm) to normalize the results and make the vessels more comparable.

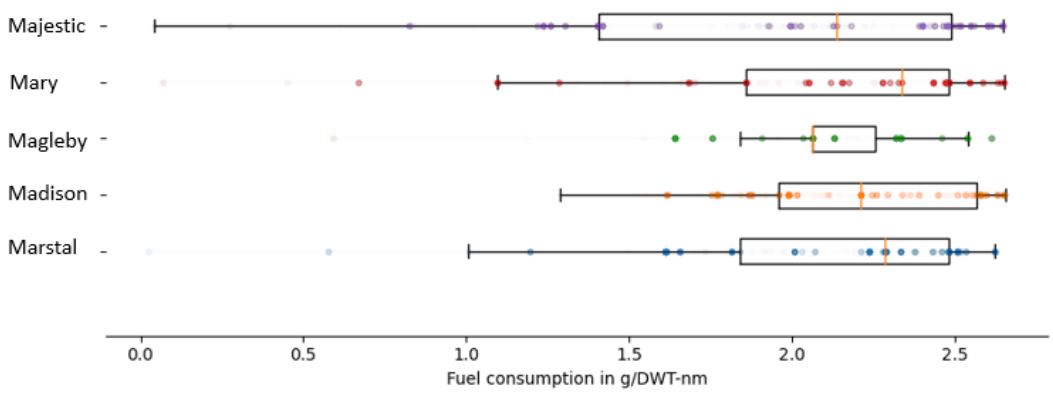

Figure 13. Box and whiskers displaying the variation in fuel consumption (g/DWT-nm) for the baseline OPs. The left end of the boxes represents the median of the lower half of the data (25th quartile), and the right end of the boxes represents the median of the upper half (75th quartile). The yellow line displays the median of the data set (50th quartile). The whiskers represent the lowest and highest data observations, excluding outliers.

The boxes in Figure 13 represent the median of the lower and upper half of the data (25th and 75th quartile, respectively), and the yellow line inside the boxes displays the median of the whole data set. All observed data points in the baseline profiles have a fuel consumption lower than three grams per transport work (represented by the whiskers). *Magleby* is the vessel with the slightest variation in fuel consumption per transport work and the lowest median data value of ~2.1 g/DWT-nm. The highest median value of ~2.4 g/DWT-nm is observed in *Mary*. The variation in observed data values is the largest for *Majestic*, with a data range between 0.1 to 2.8 g/DWT-nm.

The variation in fuel consumption within the Arctic OPs is marginal (the boxplots of the Arctic OPs can be found in *Appendix B*). In the Cv experiment, *Majestic*, *Mary,* and *Marstal* have lower fuel consumption per transport work (from ~2.0 to ~2.2 g/DWT-nm) than in the baseline. In contrast, the median fuel consumption for *Magleby* and *Madison* has not changed from the baseline. In the slow steaming OPs (Ct), the interquartile median fuel consumption has reduced further, where the vessels median data observations range from ~1.4 to ~1.8 g of fuel consumed per transport work.

The simulations in the MariTEAM model result in computations of the magnitude of emissions per species in kg each vessel is responsible for on the respective routes given the operational profiles and fuel profiles (HFO, MDO, LNG low-pressure (LP), and LNG high-pressure (HP)). Figure 15 displays the CO_2, CH_4, SO_2, and BC in metric tons emitted for the respective

experiments and vessels. Note that the scale of the y-axis differs on the respective graphs. Tables containing information about the magnitude of each emission species can be found in *Appendix C.*

Comparing the graphs in Figure 14, the largest emissions in tons are the CO_2 emissions, regardless of fuel. It is also evident that the Arctic OPs generate lower magnitudes of CO_2, SO_2, and BC emissions than the baseline OPs. Compared to the baseline, the Cv experiments simulated with HFO and MDO led to a total absolute CO_2 reduction of 11% and 13%, respectively. The Ct OPs are the experiments that generate the lowest magnitude of CO_2, SO_2, and BC emissions. The Ct experiments have a total CO_2 reduction of 29% and 31% for HFO and MDO, respectively. In the experiments run on LNG, the SO_2 and BC emissions are reduced by 99% compared to the emissions from HFO.

The experiments run on HFO and MDO generate no CH_4 emissions from combustion. The magnitude of methane (CH_4) emissions is, in contrast to the other emissions displayed in Figure 14, more prominent for the LNG OPs. The low-pressure LNG profiles have the most significant CH_4 emissions in tons, increasing with slow steaming.

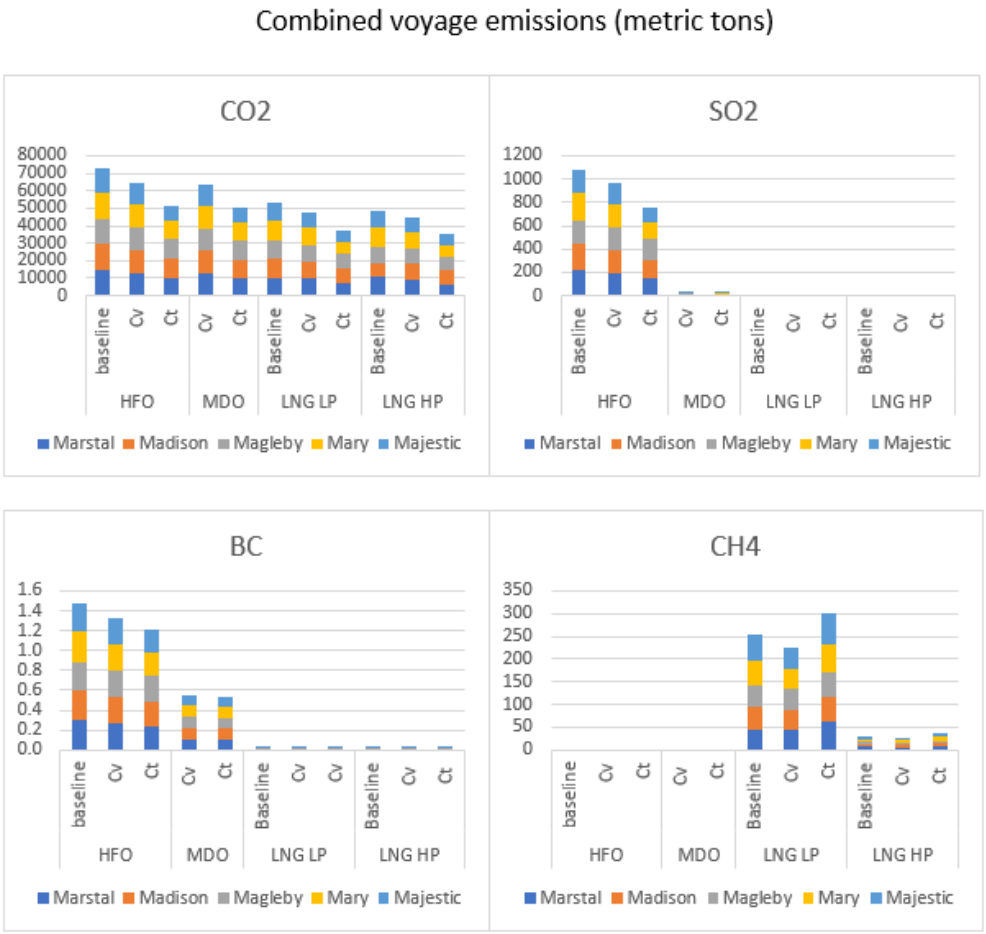

Figure 14. stacked bar chart of the total emissions associated with each vessel in each experiment in the unit of metric tons. CO_2 has the largest magnitude of emissions, followed by SO_2, CH_4 and BC. HFO has the highest CO_2, SO_2, and BC emissions, and zero emissions of CH_4.

The emission graphs above illustrate the absolute magnitude of ship emissions for the different experiments. As discussed in the introduction and method chapter, the different emission species have different properties in the atmosphere. To assess the climate impacts of the routes and operational profiles, one must normalize the emissions on a common scale. In the next section, the emissions are normalized relative to CO_2 using the climate metrics GWP and GTP.

4.4 Climate impact assessment

The global warming potential (GWP) and global temperature change potential (GTP) are aggregated for the emissions of all five vessels in the different experiments and presented in Figure 15 and Figure 16. On the x-axis of the graphs, the experiments are labeled Baseline, which is the SCR, Cv; which is the NSR with constant average speed, and Ct, which is the NSR with slow steaming. The experiments are assessed with four different fuel profiles (HFO, MDO, and LNG –

low and high pressure). The colored bars represent the climate impact of each species in kg CO_2-equivalent per DWT, and the distance sailed on each route in nautical miles. The black mark represents the net climate impact of the five one-way voyages between Shanghai and Rotterdam for the given experiment. The emission species below the horizontal line are cooling agents (NO_x, SO_2, and OC), and the species above are warming agents (CO_2, CH_4, N_2O, BC, CO). The magnitude of climate impact per emission species is listed in *Appendix D*.

4.4.1 GWP

The most significant net warming impact for each experiment (baseline, Cv and Ct) at GWP20 is observed for the experiments run on low-pressure LNG. The methane slip has an impact of 24.5 kg CO_2-eq./DWT-nm in the baseline LNG LP. The Cv LNG LP has a reduced climate impact from methane emission of -16% compared to the baseline OP on LNG LP (20.7 kg CO_2-eq./DWT-nm). In the slow steaming experiment, Ct, however, a percentage increase of 18% methane slip can be observed compared to the baseline on LNG LP (28.9 kg CO_2-eq./DWT-nm). The positive radiative forcing of methane dominates the short-term net impact of the OPs with the low-pressure LNG engine despite the relative reduction in CO_2 emissions of 31-32% compared to the HFO experiments. For the high-pressure LNG engine experiments, the methane slip is reduced by 88% relative to the LNG LP, which significantly reduces the net global warming potential.

All the experiments that run on HFO have a significant net negative climate impact at GWP20 compared to the other experiments at GWP20 and the longer time horizons (GWP100 and GTP100). The net climate impact of the HFO profiles at GWP20 is -135.5, -57.4, and -39.4 Kg CO_2-eq./DWT-nm for the baseline, Cv, and Ct, respectively. In the HFO-ban scenario, the Cv and Ct experiment exclusively run on MDO instead of HFO. SO_2 emissions are significantly reduced by 98-99% compared to the same experiments on HFO. The CO_2 emissions are reduced by 26% relative to the same experiments on HFO. The relative climate impact of BC in the MDO profiles has been reduced by 72%-74% for Cv and Ct compared to the same experiments on HFO. This result in a net positive climate impact of 9.5 and 8.1 kg CO_2-eq./DWT-nm at GWP20 for Cv and Ct, respectively, which is the second-highest short-term climate impact after LNG LP.

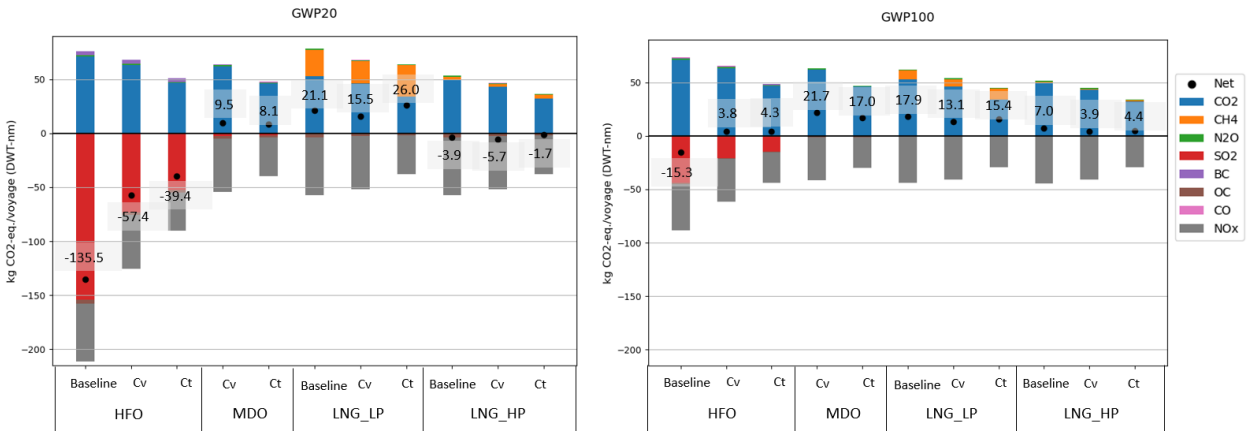

Figure 15. The stacked bar charts show the global warming potential (GWP) at TH 20 (left), and TH 100 (right) for the experiments (baseline, Cv, and Ct) run on different fuels. GWP is an integrative metric calculating the cumulative RF from a pulse emission up to a point in time.

At GWP100, the climate impact for the experiments on HFO is -15.3, 3.8, and 4.3 kg CO_2-equivalents for the baseline, Cv, and Ct, respectively, and are the operational profiles with the lowest net climate impact compared to the same OPs run on other fuels. The difference in climate impact between Cv and Ct on HFO and LNG HP is marginal, with a 0.1 kg CO_2-eq./DWT-nm difference. The GWP100 results show that the MDO-profiles yield the highest climate impact on the Arctic routes. The SO_2 emissions in Cv and Ct with MDO are -0.66 and -0.49 kg CO_2-eq./DWT-nm, which is a significant reduction compared to the same experiments on HFO (-20.71 and -14.86 kg CO_2-equivalents per/DWT-nm). The CO_2 emissions associated with the MDO profiles are more significant than those from the LNG profiles (26% larger in Cv and 31% larger in Ct). The methane slip impact in LNG LP is significantly reduced at GWP100 compared to GWP20 (-66%).

BC emissions have the highest climate impact in the HFO-experiments of 0.97, 1.01, and 0.90 kg CO_2-equivalents at GWP100 for the baseline, Cv, and Ct, respectively. The relative impact of BC increases by 5% from the baseline to Cv. The Ct experiment has a reduction of BC impact of -7%. Compared to the HFO profiles, relative BC emissions are reduced by 74-76% in the MDO profiles and 98% in the LNG profiles. The NO_x emission impact in the Cv experiments decreased by 7% compared to the baseline, and in the Ct experiments, the impact was reduced by 34% compared to the baseline. Relative to the global warming potential of carbon monoxide (CO) in the baseline OP on HFO, the impact has decreased by 1% in the slow steaming experiment (Ct) on HFO and MDO. In the Cv experiments on HFO and MDO, the relative CO climate impact is reduced by

26% compared to the baseline on HFO. All OPs run on LNG have a significant relative reduction in CO compared to the baseline on HFO (-72 to -46 %). For both GWP100 and GWP20 lowest warming potential in CO_2-eq./DWT-nm is in the baseline experiment with HFO as fuel.

4.4.2 GTP

The potential temperature change impact at year 20 and year 100 after the simulated container ship emissions in the summer of 2017 is calculated in the same unit as the GWP (kg CO_2-equivalents per transport work). GTP20 net climate impact is strongly negative for all the tested experiments. HFO has the most considerable content of SO_2, which result in additional cooling to the already strong cooling effect of NO_x emissions. The methane slip from the LNG LP engine has a temperature impact of 19.84, 16.76, and 23.36 kg CO_2-eq./DWT-nm for the baseline, Cv, and Ct, respectively, which result in LNG LP having the lowest magnitude of net cooling, compared to the same experiments run with other fuels.

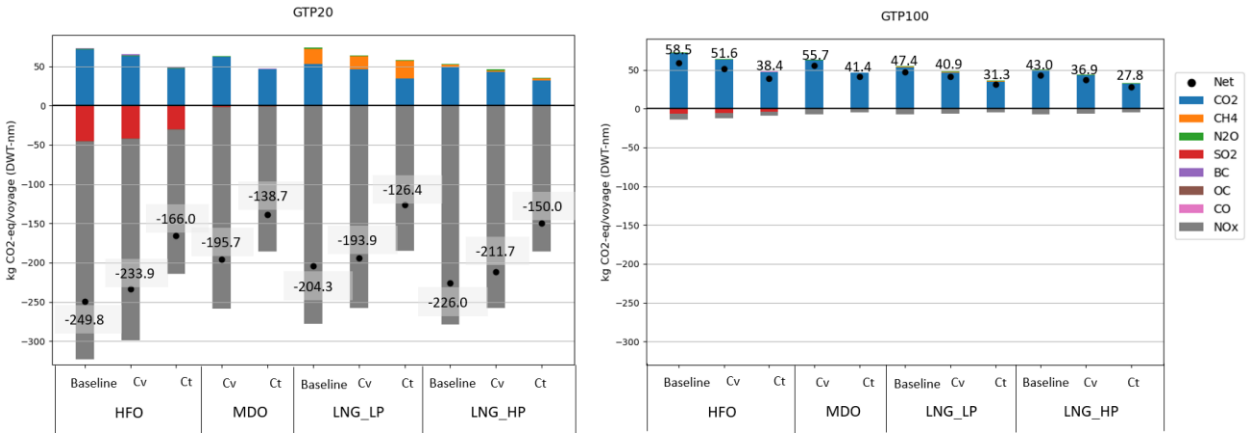

Figure 16. The stacked bar charts show the global temperature change potential (GTP) at TH 20 (left), and TH 100 (right) for the experiments (baseline, Cv, and Ct) run on different fuels. GTP is an instantaneous metric calculating the potential temperature change at a particular time in the future.

At GTP100, all experiments result in a net positive climate impact. The impact of SO_2 in the HFO experiments is reduced by 86% from GTP20 to GTP100. However, the remaining SO_2 still contributes to the Arctic experiments on HFO having a lower temperature potential than the corresponding experiments on MDO. The OPs run on LNG have the lowest temperature potential at GTP100. The CO_2 emissions per transport work have decreased by 26% for the baseline LNG LP experiment and 31% for the LNG HP experiment, relative to the baseline HFO experiment. The Cv LNG experiments have an additional -2 percentage points reduction relative

to baseline HFO. The Ct experiments have a CO_2 emission reduction of 47% and 50% for LNG LP and LNG HP, respectively, relative to the baseline HFO.

5 Discussion

Fuel consumption and fuel type, energy output, distance sailed, speed over ground, and weather affect the emissions from marine engine combustion. In this chapter, the results obtained from the MariTEAM model simulations are discussed and compared to findings in previous studies. The assumptions and the usability of the MariTEAM model for the purpose of this report are evaluated, and the potential climate change impact of the different experiments is discussed. Through the discussion, the aim is to answer the research question of whether the rerouting of vessels from the SCR to the NSR offers climate change mitigation potential and what related trade-offs the rerouting might imply.

5.1 Evaluation of the MariTEAM model and experiment assumptions

One of the main assumptions made for the simulation experiment in this report is the assumption of NSR as a perfect substitute to the SCR due to the assumption of ice-free sailing conditions and identical technical ship profiles regardless of route. This assumption is sensible when assessing the isolated climate change impact of rerouting the case vessels; however, in reality, the two routes are significantly diverse when comparing them for the purpose of container shipping. Container shipping is based on liner shipping following scheduled, fixed routes. The trading markets on the SCR are more developed and offer logistic networks that do not exist along the NSR and can likely not be replicated due to unstable ice conditions (van Hussen, 2020). Furthermore, the case vessels assessed in this study are large (DWT of above 194,000). They are designed specifically for the given route they take along the SCR, and due to areas along the NSR with shallow waters, these large vessels would not be able to navigate along the Siberian coast (Stephenson, Brigham, & Smith, 2014).

Schröder et al. (2017) emphasize the importance of ice conditions in the Arctic in their simulation study of vessels sailing through the Arctic and computes exhaust emissions given technical ship data and ice condition projection (2017). One of the main assumptions of the rerouting experiment in this report is the assumption of open water along the Siberian coast in the September month. This assumption is based on sea ice projection studies which conclude that the sea ice first retreats from near-coast areas and that the lowest ice extent is observed in September (Aksenov et al.,

2017; Melia et al., 2016). However, the ice conditions in the Arctic region are one of the greatest uncertainties regarding Trans-Arctic navigability. In a scenario where there is sea ice along the NSR in September, the case vessels would have to be escorted by an ice breaker (NSRA, 2020), which would result in additional associated exhaust emissions.

The effective power of the engine is a factor of speed and resistance (Tezdogan et al., 2016). In the Arctic OPs, the speed is constant, which means that any variation in power output is due to resistance from the weather. The time-series graphs (Figure 11 and Figure 12) show variations in weather over time on the Arctic route. Despite these variations, the vessel's fuel consumption and engine load on the Arctic routes have only marginal variations. This marginal variation could indicate that the weather data input on the Arctic route is insignificant for the vessel's fuel consumption. The Arctic operational profiles were simulated with and without the weather module to establish the difference in fuel consumption per nautical mile to assess if this was the case. When the weather is accounted for, an ~8% increase in fuel consumption per nautical mile was observed (Table 8). This weather impact is within the suggested impact range of 5-15% estimated by (Johansson et al., 2017). However, significant parts of the Arctic weather data have missing values, which are set as zero values in the model. The actual weather impact on fuel consumption could potentially be higher than the 8% accounted for in the model simulation.

Despite these limitations, the rerouting procedure and simulation results show that the MariTEAM model can be used to simulate different vessel types on alternative routes and with alternative fuels. Even though container vessels of the size used in this case study would not actually be able to navigate through the NSR, the simulation results show the relative change in emission patterns between the conventional route and the alternative Arctic route. The expanded model can be applied for any vessel type based on technical ship data from the SeaWeb^{TM} database and can easily the modified to simulate a different Arctic route by plotting different coordinates.

5.2 Implications and insight of different climate metrics

Very few studies investigating Arctic shipping have calculated the emissions reduction potential of other species than CO_2 (H. Lindstad et al., 2016; Schröder et al., 2017). The simulation results in this study show an apparent absolute emission reduction in kg of emitted species on the Arctic route (Figure 14). The total emissions of CO_2, SO_2, and BC are all reduced on the Arctic route because of the shorter travel distance. The Ct experiment shows the most significant reduction of

these emissions compared to the baseline. However, due to the difference in atmospheric properties between the different emission species (Niak et al., 2021), the absolute emission reduction is insufficient to determine the climate impact. Therefore, the GWP and GTP metrics are applied in this study to put the emissions on a common scale to compare the climate impact of the case vessels' operations on the Suez Canal Route to their simulated operations on the Northern Sea Route.

5.2.1 Differences between GWP and GTP

The main difference between the two metrics is that GWP is an integrated metric that takes the cumulative emissions over the given time horizon and thus states the additional amount of heat absorbed over a period, while the GTP is an instantaneous metric that looks at the temperature potential at a given point in the future (Shine et al., 2005; Aamaas et al., 2012). At TH 20, the cumulative climate impact of SO_2 emissions is higher than the instant impact of SO_2 20 years after the pulse emission. Figure 5 illustrates the temperature response of the different emission species at different years from emission. The figure shows that the cooling effect of SO_2 is exponentially decreasing over time and has significantly reduced at year 20 compared to the time of the pulse emission at year 0. The temperature impact of NO_x at year 20 is, however, on its maximum cooling effect, which results in the large net negative temperature impact of NO_x at GTP20 (Figure 16). The GTP results show that all the simulated experiments have a net negative temperature potential in the short term, which switches to a net positive temperature impact in the long term, as the cooling agents have decayed at year 100. The GWP results also show an increased warming potential with time; however, the GWP100 results display the NO_x and SO_2 emissions as still impacting the energy balance by scattering incoming solar radiation. There are significant uncertainties related to GWP and GTP, such as limitations regarding the treatments of indirect effects and feedback related to emissions and geospatial variability (J. S. Fuglestvedt et al., 2010; Myhre et al., 2013b). The GTP metric has larger related uncertainties because of the additional assumptions connected to the step further on the cause-effect chain (J. S. Fuglestvedt et al., 2010).

BC, also known as soot, is a warming agent that contributes to greater warming in the Arctic region compared to lower latitudes because the soot deposited on snow and ice results in a reduced albedo effect and hence increased warming (J. S. Fuglestvedt et al., 2014; Stephenson et al., 2018). In this report, the global-mean GWP values of BC were applied to the emissions on the Suez Canal Route, and the Arctic metrics from Ødemark et al. (2012) were applied to the emissions emitted above

66.3° north on the Northern Sea Route. Thus, even though the absolute emissions of BC are reduced on the Arctic route due to lower fuel consumption, the relative climate impact of BC in CO_2-eq./DWT-nm is slightly increased in the Cv experiment when applying the GWP metric. For the GTP metric values, only global-mean values were available for all the emission species. The relative temperature impact potential of BC is thus reduced on the NSR compared to the SCR due to the reduced voyage distance.

5.2.2 Uncertainties regarding climate metric values

Short-lived climate forcers lead to a mixture of particles, making it challenging to quantify the climate impact of shipping. The global-mean impact of a year of present-day ship emissions causes short-term cooling. However, SLCFs have the most significant impacts on the local climate, and the magnitude of these local impacts is uncertain (Niak et al., 2021). NO_x is one of the most prominent emission species in the shipping sector, which becomes evident in the climate impact results, especially at TH20. NO_x emissions are, on the one hand, an ozone precursor that increases tropospheric ozone, which serves as a warming climate effect. On the other hand, NO_x reduces the lifetime and abundance of methane and thus reduces the warming effect (J. S. Fuglestvedt et al., 2010; Myhre et al., 2013b). These opposite effects result in varying magnitudes of metric value results between studies (J. S. Fuglestvedt et al., 2010; Myhre et al., 2013a). Furthermore, the location-specific metrics are subjected to uncertainty. The Arctic-specific metric values for BC, SO_2, and OC listed in the IPCC report, adopted from Ødemark et al. (2012), are, in fact, defined by the authors as global-mean values and not Arctic-specific (2012). Some scholars suggest that the location-specific metric values are too immature to apply (J. S. Fuglestvedt et al., 2010). However, the sign of the metric values is more certain, and there is a common understanding of NO_x, SO_2, and OC yielding a net negative climate impact (Niak et al., 2021).

The only previous study on Arctic shipping found applying a climate impact metric was H. Lindstad et al. (2016), investigating the climate impact of Arctic bulk shipping. H. Lindstad et al. (2016) apply the IPCC metric values (Myhre et al., 2013a) to calculate the GWP20 of shipping activity per ton transported on the NSR versus the SCR and with different fuels (LFO, MGO, and LNG HP). When comparing the metric values used in this current study to those used by H. Lindstad et al. (2016), it becomes evident that not all metric values are the same. The Arctic-specific BC metric value used by H. Lindstad et al. (2016) is more than double the Arctic BC metric value from Ødemark et al. (2012) referred to in the IPCC report and utilized in this current

study. This metric value choice leads to a significantly higher calculated BC impact on the NSR in H. Lindstad et al. (2016), compared to those calculated in this report. H. Lindstad et al. (2016) conclude that rerouting vessels to the NSR have no climate benefit because of the additional climate impacts of emissions in the Arctic. The uncertainty concerning the magnitude of metric values and the inconsistency between papers lead to uncertainty of the magnitude of climate impact from ship combustion at distinct locations.

5.3 Time and fuel savings on the NSR

The sailing distance affects the fuel consumption of a vessel; however, fuel consumption is also a function of engine load, SFOC, and speed (Tezdogan et al., 2016). The MariTEAM model simulations show that the fuel consumption and absolute emissions depend on the ME load and SFOC. *Mary* is observed to have the highest interquartile median fuel consumption in grams per transport work of all the baseline OPs, which is caused by *Mary* having the highest median load (85%), median SFOC (181.9 g/kWh), and median speed (20.1 knots). The lowest interquartile median fuel consumption is observed for *Magleby*, which has the lowest median SFOC (179.3 g/kWh), ME load (72%), and speed (19.0 knots). The boxplots of fuel consumption variation show the normalized fuel consumption of each vessel, which means that the difference in DWT and distance sailed does not affect the relative difference between the vessels. The variation in fuel consumption per transport work is thus due to variations in speed and resistance. The fuel consumption affects the magnitude of emissions, which is the lowest for *Magleby* and the highest for *Mary* (values in *Appendix C*). The models' ability to compute the relationship between speed, engine load, and SFOC makes the state-of-the-art MariTEAM simulations more advanced compared to other computational methods that do not use technical ship data, AIS data, and weather data as input.

5.3.1 The effects of shorter navigational distance

Through a model expansion of the MariTEAM model, this report presents a rerouting feature to examine whether utilizing the Northern Sea Route (NSR) as an alternative to the Suez Canal Route (SCR) for container shipping can offer climate change mitigation potential. Previous literature states that the sailing distance of the NSR between ports in North-East Asia and Northern Europe can be up to 40% shorter than the SCR, depending on the origin and end point (H. Lindstad et al., 2016; Pierre & Olivier, 2015). The average sailings distance between Shanghai and Rotterdam of the SCRs of the five case vessels simulated in the MariTEAM model is 10882 nautical miles. The

NSR is 9806 nautical miles (10% shorter than the SCR). A port such as Yokohama in Japan, which is further north and thus closer to the NSR, will have a shorter sailing distance and lower fuel consumption to Northern Europe compared to a port in Shanghai, which is located at a lower latitude (Chou, Chou, Hsu, & Lu, 2017). This explains the relatively small saving in distance in this report compared to previous literature (H. Lindstad et al., 2016; Pierre & Olivier, 2015). The time spent on the baseline voyages varies because the five case vessels took five different routes along the SCR in the summer of 2017 due to different scheduled port calls. Even though the port calls are filtered out in the baseline OPs, the vessels still take the routes reported by the AIS data. The manually plotted coordinates on the NSR are the same for all vessels. The AIS data suggests that *Magleby* sails a shorter route on the SCR than the other vessels and thus the NSR is only 4% shorter than *Magleby*'s SCR. This results in a one-day shorter voyage over the Arctic. *Mary* takes a longer route on the SCR, which results in the NSR being 13% shorter. *Mary* would thus save over four days of voyage time by taking the NSR.

The total fuel consumption in tons per voyage is reduced by 11.2% on average in the experiments with a constant average time on the Arctic route (Cv) compared to the baseline. This can be explained by the reduced navigation time, and the speed being set to the baseline average, which is close to service speed for the vessels. The engine load and SFOC are also reduced for all the vessels in the Cv experiment. The reduction in fuel consumed per voyage leads to a total reduction in aggregated CO_2 emissions of 11% in the Cv OPs run on HFO relative to the baseline on HFO.

5.3.2 Slow steaming

In the experiments with constant voyage time (Ct), the vessels arrive at Maasvlakte Port in Rotterdam at the same time as they do when taking the SCR. The vessels with the most significant percentage change in fuel consumption from Cv to Ct are the vessels with the most significant speed reduction from the average baseline speed (Cv) to the slow steaming speed. As speed is reduced in the Ct OPs, the engine loads are also reduced to a suboptimal load, which leads to higher SFOC than in the baseline OPs. Despite the increased SFOC in g/kWh, the total fuel consumption per voyage and the associated CO_2 emissions nevertheless decreases with speed reduction due to substantial resistance reduction (Tezdogan et al., 2016). The speed reduction assessed in this report is a minimum of 0.9 knots and a maximum of 4.2 knots. The Ct OPs still have speeds within the range of 15.3 to 18.1 knots, which is within the speed range in which slow steaming can be efficient (Woo & Moon, 2014). The results are coherent with the theory of slow

steaming (Armstrong, 2013; Maloni et al., 2013). On average, for all the Ct experiments run on HFO, the CO_2 emissions were reduced by 29% compared to the baseline route. The same average percentage reduction is observed for NO_x emissions. The NO_x emission factor in the MariTEAM model is constant regardless of fuel. NO_x emissions are modeled s a function of energy required by the engine and vary only depending on the vessels' operational conditions (Kramel et al., 2021). The slow steaming requires less energy (kWh), and thus less NO_x is emitted. Methane, on the other hand, increases with slow steaming. When slow steaming, the median engine loads of the vessels range between 39% to 61%, which is lower than the optimum load. The vessels with the lowest loads also have the lowest speed and the highest methane slip, which is in agreement with the theory stating that methane slip increases with incomplete combustion (E. Lindstad et al., 2020; Pavlenko et al., 2020). This report does not investigate the ideal speed for slow steaming, which could result in higher emission reductions.

The results from the slow steaming OPs show an overall reduction in total fuel consumption and emissions with reduced speed. A critique to slow steaming as an emission reduction tool is that the increased voyage time that follows may lead to a need for more ships to carry the same cargo volume over time and satisfy world trade demand. This could counter climate change mitigation (Pastra et al., 2021). However, an advantage of slow steaming through the shorter Arctic route instead of the SCR is that the vessels can arrive at the same time as scheduled on the SCR and still emit less. This would eliminate the need for additional vessels to satisfy demand.

5.4 Rerouting HFO-fuelled vessels through the Arctic

A key finding in the climate impact assessment is the net cooling climate effect of HFO. The results show that the baseline profile on HFO has the lowest climate impact of all experiments in the short-term perspective at GWP20 and GTP20 due to the significant short-term cooling effect of SO_2 and NO_x emissions. The negative metric value of SO_2 is of a lower magnitude in the Arctic than the global average value. This, combined with the lower magnitude of emissions due to a shorter route, leads to a short-term (GWP20) net increased warming potential by rerouting HFO-fuelled vessels to the Arctic relative to the SCR.

SO_2 and NO_x emissions are, however, hazardous air pollutants that, despite the cooling effect on the climate, also lead to adverse health effects and mortality (Bilsback et al., 2020). Therefore, IMO has set strict regulations on these pollutants (IMO, n.d.,-a, n.d.,-b). A concern for problem

shifting is raised about the mitigation policies implemented for these emissions because lower sulfur content in HFO leads to a relative increase in CO_2. (J. S. Fuglestvedt et al., 2014; J. S. Fuglestvedt et al., 2010). A significant difference between the Suez Canal Route and the Northern Sea Route is the human exposure potential to hazardous air pollutants. In the Arctic, the human population density is significantly lower than around the Suez Canal area, and the concern for human exposure to air pollutants in the Arctic region can therefore be considered low. A benefit of rerouting the HFO fuelled vessels to the NSR is thus the reduced human exposure to air pollutants, while the short-term cooling effect of SO_2 and NO_x is kept.

The short-term net cooling effect of HFO does not mean that increased HFO consumption is a valid climate change mitigation tool. The short-term cooling effect from HFO combustion has a high climate penalty in the long term. After one hundred years, the atmospheric impact of HFO is dominated by CO2, which persists in the atmosphere for decades and results in increased warming. From a long-term perspective, the rerouting of HFO-fuelled vessels to the Arctic will reduce climate impact due to the shorter navigational distance. At GTP100, the combination of shorter navigational distance on the NSR and fuel savings with slow steaming leads to a temperature change potential reduction of -20.1 kg CO_2-equivalents per transport work when rerouting from the SCR to the NSR. Hence, the isolated climate impact of rerouting HFO-fuelled vessels to the Arctic is eventually a net reduction in temperature impact. However, the climate impact assessment does not consider other environmental aspects of HFO, such as the potential impacts of an oil spill. HFO-spills are more persistent in the water than distillate fuels and are almost impossible to clean up (Comer, 2019). This risk is one of the reasons why the IMO has adopted an HFO-ban in the Arctic, which will take effect in 2024 (IMO, 2020).

5.5 Implications of an Arctic HFO-ban

The climate effects of the HFO-ban are assessed by simulating the vessels with MDO as fuel exclusively in the Arctic. The economic aspect of rerouting is not the focus of this report; however, it is worth noting that MDO is a more expensive fuel than HFO (DNV, 2019). For Arctic rerouting to be economically feasible, the benefit of fuel savings must exceed the additional fuel costs. The HFO-ban may thus serve as an economic barrier for Arctic shipping, as long as HFO is the dominant marine fuel in the rest of the world.

The MDO has a lower sulfur and carbon content than HFO, which lead to two opposite climate effects due to SO_2 being a cooling agent and CO_2 being a warming agent. Compared to the Arctic experiments on HFO, the MDO experiments lead to increased net climate impact regardless of the time horizon, and the metric used because the reduction in SO_2 is significantly larger than the relative reduction in CO_2 emissions. Hence, the isolated short-term (GWP20) climate effect of switching to MDO in the Arctic is increased net warming compared to the climate effects of HFO-fuelled vessels in the Arctic. These results are, however, only considering direct climate impacts of emissions to air, which does not include the risk of an oil spill and its potential feedback effect regarding reduced albedo effects. A more holistic analysis accounting for these aspects may result in a different environmental impact result.

The HFO-ban may be expanded to include a ban on MDO (Comer, 2019). In that case, LNG is the alternative fuel investigated in this report. From a climate impact perspective, LNG as fuel in both main and auxiliary engines has the potential for significant global warming and temperature reduction compared to MDO at TH100 due to significantly lower carbon content. However, the choice of LNG engine type is crucial for the potential climate change mitigation, especially in the short term. The climate impact results show a significantly higher methane slip in the low-pressure (LP) LNG profiles than in the high-pressure (HP) LNG profiles. In the short-run (GWP20), a switch to LNG LP from MDO increases CO_2-equivalents by 64%. A switch to LNG HP leads to a reduction of 160% in CO_2-equivalents. Hence, due to the large methane slip from the low-pressure engine, the short-term impact of LNG LP is increased warming compared to the MDO-fuelled Arctic operational profiles. The high-pressure LNG engine leads to significantly lower methane slip, which results in a lower net impact than the net impact of MDO in the short-term and the long-term.

Compared to the baseline HFO profile, the short-term impact of rerouting LNG-fuelled vessels through the NSR is increased warming and temperature potential due to lower emissions of cooling agents and higher emissions of the warming methane. However, in a long-term perspective, when SO_2, NO_x, and CH_4 have significantly decayed, the benefit of the low carbon content in LNG becomes evident. Thus, the OPs with the lowest fuel consumption and carbon content are to OPs with the largest climate change mitigation potential.

5.6 Global transition towards low carbon fuels

For the shipping sector to reach the IMO goal of phasing out GHG emissions in this century (IMO, n.d,), vessels must run on alternative fuels to HFO, not only in the Arctic. Carbon-neutral fuels such as hydrogen and ammonia are currently being tested but are not yet commercialized (Wärtsilä, 2021). Furthermore, the price of carbon-neutral fuels is expected to be high, while the price of LNG has been expected to be competitive with the price of low-sulfur HFO (DNV, 2019). This is, however, subject to considerable uncertainties following the energy crisis and increased gas prices after the Russian invasion of Ukraine (Stevens, 2022). Regardless, LNG is the fuel that currently dominates the alternative fuel segment (DNV, 2021) and could potentially be the most available option at the beginning of the fuel transition, as the switch to LNG from HFO is possible with retrofitting of fuel- and engine systems. LNG can be used directly in duel-fuel engines (E. Lindstad et al., 2020), with which the case vessels are already equipped. The baseline OPs were simulated with LNG as fuel to investigate such a fuel transition scenario and compare the climate change impact of rerouting vessels through the NSR when HFO is no longer a fuel option.

A key finding in the impact assessment is the difference in impact results depending on time horizon and climate metric. On the time horizon of 20 years, the methane slip is more significant than in year 100 due to the short lifetime of CH_4. In the short run, the GWP results suggest that rerouting of LNG-fuelled vessels to the NSR with slow steaming leads to an increase in global warming potential due to increased methane slip with incomplete combustion. The warming impact of methane slip thus offsets the effect of reduced fuel consumption due to reduced navigational distance. At GWP100, when the CH_4 has decayed, the rerouting from SCR to NSR results in reduced warming potential; however, the slow steaming experiment still has a larger climate impact than the experiment with constant average speed. The calculated temperature potential at year 100 (GTP100) shows a significant reduction in CO_2-equivalents per transport work on the Arctic route regardless of speed profile (Cv or Ct) and LNG engine (HP or LP). The fuel savings from the shorter Arctic navigation distance lead to long-term climate change mitigation potential of rerouting the LNG-fuelled case vessels from the SCR to the NSR.

5.7 Outlook and further research

The MariTEAM model is a state-of-the-art emissions assessment model that assesses the emissions associated with actual, historical voyages based on AIS data, technical ship data, and weather data. The rerouting procedure developed for the MariTEAM model in this thesis can be subject to further

research on emissions associated with other vessel types or other Arctic routes. A limitation to the MariTEAM Arctic re-routing procedure is the uncertainties related to ice extent and thickness and its impact on fuel consumption. Further research is suggested to assess the possibility of extending the weather input data to account for resistance due to ice conditions to refine the expanded MariTEAM model and better account for weather in the Arctic.

This thesis shows that rerouting from the SCR to the NSR is beneficial in terms of global emissions reduction due to the shorter distance from the origin to the destination. The Arctic route simulations in this report lead to a 10% shorter navigational distance, which is a lower reduction than in previous studies between other ports (H. Lindstad et al., 2016; Pierre & Olivier, 2015; Schröder et al., 2017; Schøyen & Bråthen, 2011). As the ice extent is expected to decrease further at mid-century (Aksenov et al., 2017; Melia et al., 2016), shorter Arctic routes across the central Arctic are expected to open, which will lead to shorter navigational distances between Asia and Europe than what the NSR is computed to provide in this report. This will result in additional global climate change mitigation potential of rerouting, as lower fuel consumption results in lower long-term climate impact from the long-lasting CO_2 emissions. However, the rerouting implies an increase in local emissions in the Arctic. From this report's results, it is unclear if the assitional local long-term warming will lead to feedback loops that offset the benefits of reduced global climate impact. Other environmental aspects beyond the isolated climate change impacts are thus of interest for further research, such as the impact of increased Arctic activity on biodiversity and the permafrost.

6 Conclusion

The objective of this thesis was to expand the state-of-the-art tank-to-wake emission assessment MariTEAM model with a rerouting feature to simulate vessels from the global fleet through the Arctic. Based on historical AIS and technical ship data, five container vessels from Maersk were simulated on an alternative Arctic route along the Northern Sea Route (NSR). The vessels' origin (Shanghai) and destination (Rotterdam) were set equal to the observed coordinates from the historical AIS data, and the coordinate points on the route were manually plotted. Two experiments were conducted on the Arctic route, (1) simulating the vessels with a constant speed equal to the average speed of the vessels on the Suez Canal Route (SCR), and (2) simulating the vessels with a voyage duration equal to the SCR voyage (i.e., allowing for slow steaming). The rerouting

procedure developed in this thesis contributes to the development of the MariTEAM model. It attempts to extend the usability of the model from purely historical emissions modeling to include a feature for alternative route comparisons. Moreover, the model modification resulted in further knowledge about the MariTEAM model and its strengths and weaknesses.

The combination of bottom-up ship emissions modeling and climate impact assessments is valuable for better insight into the climate impact of different ship emissions. The main research question was whether the rerouting from the SCR to the NSR offers climate change mitigation potential and what related trade-offs a rerouting could imply. This was assessed by comparing the global warming potential (GWP) and global temperature change potential (GTP) of the five case vessels on the two different routes with different fuel profiles. The climate impact results depended heavily on the time horizon and fuel profile. Short-term climate metrics show a significant net negative temperature impact of shipping due to sizeable short-term cooling effects of NO_x and SO_2. The lower fuel consumption and overall emissions on the NSR reduce this short-term cooling effect relative to the Suez Canal route. However, the shorter navigational distance also leads to long-lived GHG emission reduction for all fuels and operational profiles in the long term. The results imply that LNG is the best fuel option compared to HFO and MDO in terms of kg CO_2-equivalents per nautical mile. Combining low-carbon fuels and rerouting from the conventional SCR to the NSR will result in significant global climate change mitigation potential. However, a significant trade-off associated with rerouting is the increased local warming implied by increased Arctic activity. Additional Arctic warming risks feedback loops related to impacts on biodiversity and the permafrost, which are indirect impacts from exhaust emissions not captured by the GWP and GTP metrics.

Bibliography

Aksenov, Y., Popova, E. E., Yool, A., Nurser, A. G., Williams, T. D., Bertino, L., & Bergh, J. (2017). On the future navigability of Arctic sea routes: High-resolution projections of the Arctic Ocean and sea ice. *Marine Policy, 75*, 300-317.

Ananth, T. (Producer). (2021). 3 Important Calculations Every Marine Engineer Must Know On Ships. Retrieved from https://www.marineinsight.com/guidelines/3-important-calculations-every-marine-engineer-must-know/

Armstrong, V. N. (2013). Vessel optimisation for low carbon shipping. *Ocean Engineering, 73*, 195-207.

Balcombe, P., Brierley, J., Lewis, C., Skatvedt, L., Speirs, J., Hawkes, A., & Staffell, I. (2019). How to decarbonise international shipping: Options for fuels, technologies and policies. *Energy conversion and management, 182*, 72-88.

Bilsback, K. R., Kerry, D., Croft, B., Ford, B., Jathar, S. H., Carter, E., . . . Pierce, J. R. (2020). Beyond SOx reductions from shipping: assessing the impact of NOx and carbonaceous-particle controls on human health and climate. *Environmental Research Letters, 15*(12), 124046.

Chou, M.-T., Chou, T.-Y., Hsu, Y.-R., & Lu, C.-P. (2017). Fuel consumption ratio analysis for transiting from various ports and harbours in Asia through the Northern Sea Route. *The Journal of Navigation, 70*(4), 859-869.

Collins, W. D., Liao, H., Adhikary, B., Artaxo, P., Berntsen, T., Fuzzi, S., . . . Zanis, P. (2019). *Short-lived climate forcers. In Climate Change 2021: The Physical Science Basis. Contribution of Working Group I to the Sixth Assessment Report of the Intergovernmental Panel on Climate Change*. Retrieved from https://www.ipcc.ch/report/ar6/wg1/downloads/report/IPCC_AR6_WGI_FOD_Chapter06.pdf

Comer, B. (2019). Transitioning away from heavy fuel oil in Arctic shipping. *International Council on Clean Transportation working paper, 3*.

DNV. (2019). *Assessment of selected alternative fuels and technologies*. Retrieved from https://www.dnv.com/publications/assessment-of-selected-alternative-fuels-and-technologies-rev-june-2019--116334

DNV. (2021). *DNV Maritime Forecast 2050*. Retrieved from https://eto.dnv.com/2021/maritime-forecast-2050/about

ECMWF. (n.d.,). ECMWF Reanalysis - Interim (ERA-Interim). Retrieved from https://www.ecmwf.int/en/forecasts/dataset/ecmwf-reanalysis-interim

El-Taybany, A., Moustafa, M., Mansour, M., & Tawfik, A. A. (2019). Quantification of the exhaust emissions from seagoing ships in Suez Canal waterway. *Alexandria Engineering Journal, 58*(1), 19-25.

Faber, J., Hanayama, S., Zhang, S., Pereda, P., Comer, B., Hauerhof, E., & Yuan, H. (2020). Fourth IMO greenhouse gas study. *Retrieved from the International Maritime Organization website: https://docs. imo. org*.

Fox-Kemper, B., Hewitt, H. T., Xiao, C., Aðalgeirsdóttir, G., Drijfhout, S. S., Edwards, T. L., . . . Yu, Y. (2021). *Ocean, Cryosphere and Sea Level Change. In Climate Change 2021: The Physical Science Basis. Contribution of Working Group I to the Sixth Assessment Report of the Intergovernmental Panel on Climate Change*

Retrieved from https://www.ipcc.ch/report/ar6/wg1/downloads/report/IPCC_AR6_WGI_Chapter_09.pdf

Fuglestvedt, J., Berntsen, T., Myhre, G., Rypdal, K., & Skeie, R. B. (2008). Climate forcing from the transport sectors. *Proceedings of the national academy of sciences, 105*(2), 454-458.

Fuglestvedt, J. S., Dalsøren, S. B., Samset, B. H., Berntsen, T., Myhre, G., Hodnebrog, Ø., . . . Bergh, T. F. (2014). Climate penalty for shifting shipping to the Arctic. *Environmental Science & Technology, 48*(22), 13273-13279.

Fuglestvedt, J. S., Shine, K. P., Berntsen, T., Cook, J., Lee, D., Stenke, A., . . . Waitz, I. (2010). Transport impacts on atmosphere and climate: Metrics. *Atmospheric Environment, 44*(37), 4648-4677.

Gasser, T., Peters, G. P., Fuglestvedt, J. S., Collins, W. J., Shindell, D. T., & Ciais, P. (2017). Accounting for the climate–carbon feedback in emission metrics. *Earth System Dynamics, 8*(2), 235-253.

Goldsworthy, L., & Goldsworthy, B. (2015). Modelling of ship engine exhaust emissions in ports and extensive coastal waters based on terrestrial AIS data–An Australian case study. *Environmental Modelling & Software, 63*, 45-60.

IHS Maritime & Tarde. (n.d.,). Sea-web™ Ships. The Ultimate Maritime Reference Tool. Retrieved from https://maritime.ihs.com/EntitlementPortal/Home/Information/Seaweb_Ships#verticalTab3

IMO. (2020). Prevention and Response (PPR 7), 17-21 February 2020. Retrieved from https://www.imo.org/en/MediaCentre/MeetingSummaries/Pages/PPR-7th-Session.aspx

IMO. (n.d,). IMO's work to cut GHG emissions from ships [Press release]. Retrieved from https://www.imo.org/en/MediaCentre/HotTopics/Pages/Cutting-GHG-emissions.aspx

IMO (Producer). (n.d., 07.05.22). AIS transponders

IMO. (n.d.,-a). Nitrogen Oxides (NOx) – Regulation 13. Retrieved from https://www.imo.org/en/OurWork/Environment/Pages/Nitrogen-oxides-(NOx)-%E2%80%93-Regulation-13.aspx

IMO. (n.d.,-b). Sulphur oxides (SOx) and Particulate Matter (PM) – Regulation 14. Retrieved from https://www.imo.org/en/OurWork/Environment/Pages/Sulphur-oxides-(SOx)-%E2%80%93-Regulation-14.aspx

Jalkanen, J.-P., Johansson, L., Kukkonen, J., Brink, A., Kalli, J., & Stipa, T. (2012). Extension of an assessment model of ship traffic exhaust emissions for particulate matter and carbon monoxide. *Atmospheric Chemistry and Physics, 12*(5), 2641-2659.

Johansson, L., Jalkanen, J.-P., & Kukkonen, J. (2017). Global assessment of shipping emissions in 2015 on a high spatial and temporal resolution. *Atmospheric Environment, 167*, 403-415.

Kramel, D., Muri, H., Kim, Y., Lonka, R., Nielsen, J. B., Ringvold, A. L., . . . Strømman, A. H. (2021). Global Shipping Emissions from a Well-to-Wake Perspective: The MariTEAM Model. *Environmental Science & Technology*.

Kwon, Y., Lim, H., Lim, Y., & Lee, H. (2019). Implication of activity-based vessel emission to improve regional air inventory in a port area. *Atmospheric Environment, 203*, 262-270.

Lee, J. M.-y., & Wong, E. Y.-c. (2021). *Suez Canal blockage: an analysis of legal impact, risks and liabilities to the global supply chain.* Paper presented at the MATEC Web of Conferences.

Lenton, T. M., Rockström, J., Gaffney, O., Rahmstorf, S., Richardson, K., Steffen, W., & Schellnhuber, H. J. (2019). Climate tipping points—too risky to bet against. In: Nature Publishing Group.

Lindstad, E., Eskeland, G. S., Rialland, A., & Valland, A. (2020). Decarbonizing maritime transport: The importance of engine technology and regulations for LNG to serve as a transition fuel. *Sustainability, 12*(21), 8793.

Lindstad, H., Bright, R. M., & Strømman, A. H. (2016). Economic savings linked to future Arctic shipping trade are at odds with climate change mitigation. *Transport Policy, 45*, 24-30.

Lund, M. T., Aamaas, B., Stjern, C. W., Klimont, Z., Berntsen, T. K., & Samset, B. H. (2020). A continued role of short-lived climate forcers under the Shared Socioeconomic Pathways. *Earth System Dynamics, 11*(4), 977-993.

Maersk (Producer). (n.d.,). Schedules - Point to point Retrieved from https://www.maersk.com/schedules/pointToPoint

Maloni, M., Paul, J. A., & Gligor, D. M. (2013). Slow steaming impacts on ocean carriers and shippers. *Maritime Economics & Logistics, 15*(2), 151-171.

MarineTraffic. (n.d.,). Live Map. Retrieved from https://www.marinetraffic.com/en/ais/home/centerx:62.4/centery:36.3/zoom:2. https://www.marinetraffic.com/en/ais/home/centerx:62.4/centery:36.3/zoom:2

Melia, N., Haines, K., & Hawkins, E. (2016). Sea ice decline and 21st century trans-Arctic shipping routes. *Geophysical research letters, 43*(18), 9720-9728.

Meredith, M., M. Sommerkorn, S. Cassotta, C. D., A. Ekaykin, A. Hollowed, G. Kofinas, . . . E.A.G. Schuur. (2019). *Polar Regions.* . Retrieved from https://www.ipcc.ch/site/assets/uploads/sites/3/2019/11/07_SROCC_Ch03_FINAL.pdf

Mladek, R. (2019, 15.03.2019). Encoding details Retrieved from https://confluence.ecmwf.int/display/WLW/Encoding+details

Myhre , G., Shindell, D., Bréon, F.-M., Collins, W., Fuglestvedt, J., Huang, J., . . . Zhang, H. (2013a). *2013: Anthropogenic and Natural Radiative Forcing Supplementary Material*. Retrieved from https://www.ipcc.ch/site/assets/uploads/2018/07/WGI_AR5.Chap_.8_SM.pdf

Myhre , G., Shindell, D., Bréon, F.-M., Collins, W., Fuglestvedt, J., Huang, J., . . . Zhang, H. (2013b). *2013: Anthropogenic and Natural Radiative Forcing. In: Climate Change 2013: The Physical Science Basis. Contribution of Working Group I to the Fifth Assessment*

Report of the Intergovernmental Panel on Climate Change. Retrieved from

Niak, V., Szopa, S., Adhikary, B., Artaxo, P., Berntsen , T., Collins, W. D., . . . Unger, N. (2021). *Short-Lived Climate Forcers*. Retrieved from https://www.ipcc.ch/report/ar6/wg1/downloads/report/IPCC_AR6_WGI_Chapter_06.pdf

NSRA. (2020). *Rules of navigation in the water area of the Northen Sea Route*. Russian Federation Govenrment Decree Retrieved from http://www.nsra.ru/files/fileslist/137-en5894-2020-11-19_rules.pdf

NTNU (Producer). (n.d,). Industrial Ecology Programme Retrieved from https://www.ntnu.edu/indecol/industrial-ecology-programme

Nunes, R., Alvim-Ferraz, M., Martins, F., & Sousa, S. (2017). The activity-based methodology to assess ship emissions-A review. *Environmental Pollution, 231*, 87-103.

Parker, S., Raucci, C., Smith, T. W. P., & Laffineur, L. (2015). Understanding the Energy Efficiency Operational Indicator: An empirical analysis of ships from the Royal Belgian Shipowners' Association. Retrieved from https://www.seacargocharter.org/wp-content/uploads/2020/10/UCL-2015-Understanding-the-Energy-Efficiency-Operational-Indicator-Main.pdf

Pastra, A., Zachariadis, P., & Alifragkis, A. (2021). The Role of Slow Steaming in Shipping and Methods of CO 2 Reduction. In *Sustainability in the Maritime Domain* (pp. 337-352): Springer.

Pathak, M., Slade, R., Pichs-Madruga, R., Vorsatz, D. Ü., Shukla, P. R., & Skea, J. (2021). Technical Summary. In Climate Change 2021: Mitigation of Climate Change. Contribution of Working Group III to the Sixth Assessment Report of the Intergovernmental Panel on Climate Change. Retrieved from https://report.ipcc.ch/ar6wg3/pdf/IPCC_AR6_WGIII_FinalDraft_TechnicalSummary.pdf

Pavlenko, N., Comer, B., Zhou, Y., Clark, N., & Rutherford, D. (2020). The climate implications of using LNG as a marine fuel. *International Council on Clean Transportation: Berlin, Germany*.

Peters, G. P., Aamaas, B., T. Lund, M., Solli, C., & Fuglestvedt, J. S. (2011). Alternative "global warming" metrics in life cycle assessment: a case study with existing transportation data. *Environmental Science & Technology, 45*(20), 8633-8641.

Pierre, C., & Olivier, F. (2015). Relevance of the Northern Sea Route (NSR) for bulk shipping. *Transportation Research Part A: Policy and Practice, 78*, 337-346.

Ritchie, H., & Roser, M. (2020). CO_2 and Greenhouse Gas Emissions: Emissions by sector. Retrieved from https://ourworldindata.org/emissions-by-sector. Retrieved 03.05.22 https://ourworldindata.org/emissions-by-sector

SCA. (n.d,). Navigation Statistics. Yearly statistics. Retrieved from https://www.suezcanal.gov.eg/English/Navigation/Pages/NavigationStatistics.aspx. Retrieved 19.01.2022, from Suez Canal Authority https://www.suezcanal.gov.eg/English/Navigation/Pages/NavigationStatistics.aspx

Schröder, C., Reimer, N., & Jochmann, P. (2017). Environmental impact of exhaust emissions by Arctic shipping. *Ambio, 46*(3), 400-409.

Schøyen, H., & Bråthen, S. (2011). The Northern Sea Route versus the Suez Canal: cases from bulk shipping. *Journal of Transport Geography, 19*(4), 977-983.

Shine, K. P., Fuglestvedt, J. S., Hailemariam, K., & Stuber, N. (2005). Alternatives to the global warming potential for comparing climate impacts of emissions of greenhouse gases. *Climatic Change, 68*(3), 281-302.

Smith, T. W. P., Jalkanen, J. P., Anderson, B. A., Corbett, J. J., Faber, J., Hanayama, S., . . . Aldous, L. e. a. (2015). *Third IMO Greenhouse Gas Study 2014*. Retrieved from London, UK:

Stephenson, S. R., Brigham, L. W., & Smith, L. C. (2014). Marine accessibility along Russia's Northern Sea route. *Polar Geography, 37*(2), 111-133.

Stephenson, S. R., Wang, W., Zender, C. S., Wang, H., Davis, S. J., & Rasch, P. J. (2018). Climatic responses to future trans-Arctic shipping. *Geophysical research letters, 45*(18), 9898-9908.

Stevens, P. (2022, 18 April 2022). Natural gas surges to highest level since 2008 as Russia's war upends energy markets. *CNBC*. Retrieved from https://www.cnbc.com/2022/04/18/natural-gas-surges-to-highest-level-since-2008-as-russias-war-upends-energy-markets.html

Sun, Y., Yang, L., & Zheng, J. (2020). Emission control areas: More or fewer? *Transportation Research Part D: Transport and Environment, 84*, 102349.

Tezdogan, T., Incecik, A., Turan, O., & Kellett, P. (2016). Assessing the impact of a slow steaming approach on reducing the fuel consumption of a containership advancing in head seas. *Transportation Research Procedia, 14*, 1659-1668.

Theocharis, D., Pettit, S., Rodrigues, V. S., & Haider, J. (2018). Arctic shipping: A systematic literature review of comparative studies. *Journal of Transport Geography, 69*, 112-128.

Tichavska, M., & Tovar, B. (2015). Port-city exhaust emission model: An application to cruise and ferry operations in Las Palmas Port. *Transportation Research Part A: Policy and Practice, 78*, 347-360.

Tiseo, I. (2021). Distribution of carbon dioxide emissions produced by the transportation sector worldwide in 2020, by subsector. Retrieved from https://www.statista.com/statistics/1185535/transport-carbon-dioxide-emissions-breakdown/. Retrieved 07.02.2022 https://www.statista.com/statistics/1185535/transport-carbon-dioxide-emissions-breakdown/

UNCTAD. (2018). Review of Maritime Transport 2018. Retrieved from https://unctad.org/system/files/official-document/rmt2018_en.pdf

UNCTAD. (2020). Review of Maritime Transport 2020. Retrieved from https://unctad.org/topic/transport-and-trade-logistics/review-of-maritime-transport

UNFCCC. (2015). *Decisions adopted by the Conference of the Parties*. Paper presented at the United Nations Framework Convention on Climate Change, Paris. https://unfccc.int/resource/docs/2015/cop21/eng/10a01.pdf

van Hussen, K. (2020). *Commercial Navigation Along the Northern Sea Route: Prospects and Impacts*. Retrieved from Paris: https://www.itf-oecd.org/sites/default/files/docs/commercial-shipping-northern-sea-route.pdf

Weng, J., Shi, K., Gan, X., Li, G., & Huang, Z. (2020). Ship emission estimation with high spatial-temporal resolution in the Yangtze River estuary using AIS data. *Journal of Cleaner Production, 248*, 119297.

Winebrake, J. J., Corbett, J. J., & Meyer, P. E. (2007). Energy use and emissions from marine vessels: a total fuel life cycle approach. *Journal of the Air & Waste Management Association, 57*(1), 102-110.

WMO. (2021). WMO recognizes new Arctic temperature record of 38°C [Press release]. Retrieved from https://public.wmo.int/en/media/press-release/wmo-recognizes-new-arctic-temperature-record-of-38%E2%81%B0c

Woo, J.-K., & Moon, D. S.-H. (2014). The effects of slow steaming on the environmental performance in liner shipping. *Maritime Policy & Management, 41*(2), 176-191.

Wärtsilä. (2021). Wärtsilä launches major test programme towards carbon-free solutions with hydrogen and ammonia [Press release]. Retrieved from https://www.wartsila.com/media/news/14-07-2021-wartsila-launches-major-test-programme-towards-carbon-free-solutions-with-hydrogen-and-ammonia-2953362

Xu, H., & Yang, D. (2020). LNG-fuelled container ship sailing on the Arctic Sea: Economic and emission assessment. *Transportation Research Part D: Transport and Environment, 87*, 102556.

Zhao, H., & Hu, H. (2016). Study on Economic Evaluation of the Northern Sea Route: Taking the Voyage of Yong Sheng as an Example. *Transportation Research Record, 2549*(1), 78-85. doi:10.3141/2549-09

Zheng, C., Xiao, Z., Zhou, W., Chen, X., & Chen, X. (2018). Characteristics of Important Routes, Channels, and Ports. In *21st Century Maritime Silk Road: A Peaceful Way Forward* (pp. 87-104): Springer.

Ødemark, K., Dalsøren, S., Samset, B., Berntsen, T., Fuglestvedt, J., & Myhre, G. (2012). Short-lived climate forcers from current shipping and petroleum activities in the Arctic. *Atmospheric Chemistry and Physics, 12*(4), 1979-1993.

Aamaas, B., Peters, G., & Fuglestvedt, J. (2012). A synthesis of climate-based emission metrics with applications. *Earth Syst. Dynam. Discuss, 3*, 871-934.

Appendices

Appendix A: Python Codes

The MariTEAM model code was filtered and modified to simulate a one-way voyage from Shanghai to Rotterdam in 2017. In addition to the Baseline OP (appendix section A.1), an alternative Arctic route simulation was developed (appendix section A.2).

A.1: Clean-up baseline OPs

The below code is developed to clean up the original operational profiles retrieved from the MariTEAM model, in order to only investigate a one-way voyage between Shanghai and Rotterdam in the summer of 2017.

```
import pandas as pd
import geopandas as gpd
import matplotlib.pyplot as plt
from datetime import datetime
import numpy as np
import constants as constants

# open a result csv obtained from run_model.py
op = pd.read_csv('data/maersk china_netherlands/MADISON_219018864.csv')
op = op.drop(op.index[op['unixtimestamp'] < 1496268000]) #filter out activity
before June 1st
op = op.sort_values(by='unixtimestamp')
op['delta_dist_km'].replace('', np.nan, inplace=True)
op.dropna(subset=['delta_dist_km'], inplace=True)
op.reset_index(inplace=True, drop=True)
mmsi =219018864

# remove all points outside before Yanshan Port and after Maasvlakte Port
lat = op['y']
lon = op['x']

drop_lon = 117.5
drop_lat = 30.6254
list_drop = []
for i in range(len(op)):
    if op['y'][i] > drop_lat and op['x'][i] > drop_lon:
        list_drop.append(i)
op.reset_index(inplace=True, drop=True)
op.drop(list_drop, axis=0, inplace=True)

drop_lon2 = 4.1
drop_lat2 = 52.1
list_drop2 = []
lat = op['y'].tolist()
lon = op['x'].tolist()
for i in range(len(op)):
    if lat[i] > drop_lat2 and lon[i] > drop_lon2:
        list_drop2.append(i)
op.reset_index(inplace=True, drop=True)
```

```
op.drop(list_drop2, axis=0, inplace=True)

# Yanshan area
min_lat = 30.6253
max_lat = 30.6254
min_lon = 122.049
max_lon = 122.05
count = 0
#for n in range(count):
for i in range(len(op)):
    if min_lat <= lat[i] <= max_lat:
        if min_lon <= lon[i] <= max_lon:
            res = op.iloc[i:]
            count += 1
            if count == 2:
                break
print(res)
res.to_csv('data/test_baseline.csv')
df = pd.read_csv('data/test_baseline.csv')
lat = df['y']
lon = df['x']
# Maasvlakte area
min_lat = 52.0
max_lat = 52.01
max_lon = 4.01
min_lon = 4.0
for i in range(len(df)):
    if min_lat <= lat[i] <= max_lat:
        if min_lon <= lon[i] <= max_lon:
            res = df.iloc[:i]
            break
res.to_csv('data/baseline.csv')

op1 = pd.read_csv('data/baseline.csv')
op1 = op1.drop(op1.index[op1['sog'] == 0])
#op = op.sort_values(by='unixtimestamp')
op1.reset_index(inplace=True)
#create new delta_time_s
op1['sog_km'] = op1['sog'] * constants.KMS_KN
delta_time_s = op1['delta_dist_km'] / op1['sog_km']
op1['delta_time_s'] = delta_time_s

#unixtimestamp correlated with delta_time_s
timestamp = op1['unixtimestamp'][0]
unixtimestamp=[timestamp]
for i in range(1,len(op1)):
    timestamp += delta_time_s[i]
    unixtimestamp.append(timestamp)

op1['unixtimestamp'] = unixtimestamp
op1['reefer_main'] = 'TRUE'

op1.drop(op1.columns[op1.columns.str.contains('unnamed',case = False)],axis =
1, inplace = True)
print(op1)
op1.to_csv('data/Baselines/'+str(mmsi)+'_baseline.csv')
```

A.2: Arctic route procedure

The following code is developed for plotting the Arctic route all the vessels follow.

```
from pyproj import Geod, geod
import pandas as pd

g = Geod(ellps='clrk66') # Use Clarke 1866 ellipsoid.
# specify the lat/lons of some locations.
yangshan_lat = 30.6211; yangshan_lon = 122.0647
sea_of_jap_lat = 34.4883; sea_of_jap_lon = 129.9463
tsugaru_lat = 41.6072; tsugaru_lon = 140.8447
erimomisaki_lat = 41.6072; erimomisaki_lon = 143.2672
stillehavet_lat = 51.3992; stillehavet_lon = 159.4335
transit_ko_at_lat = 55.7518; transit_ko_at_lon = 164.7070
lawrence_island_lat =64.0866; lawrence_island_lon = -172.6727
chukchi_sea_lat =66.2580; chukchi_sea_lon = -169.0031
wrangel_lat = 70.5980; wrangel_lon = 177.0996
kotelny_island_lat = 74.5199; kotelny_island_lon = 148.3593
laptev_lat = 81.7484; laptev_lon = 95.0976
vilkitsky_lat = 80.8309; vilkitsky_lon = 83.2303
kara_sea_lat =77.5041; kara_sea_lon = 70.8398
mehamn_lat = 71.5040; mehamn_lon = 27.4219
norwegian_sea_lat = 70.0656; norwegian_sea_lon = 14.9414
north_sea_lat = 61.8561; north_sea_lon = 3.8671
nieuwe_waterweg_lat = 51.9984; nieuwe_waterweg_lon = 4.0292

#make list of longitude (x) and latitude (y):
x = [yangshan_lon, sea_of_jap_lon, tsugaru_lon, erimomisaki_lon,
stillehavet_lon, transit_ko_at_lon, lawrence_island_lon, chukchi_sea_lon,
wrangel_lon, kotelny_island_lon, laptev_lon, vilkitsky_lon, kara_sea_lon,
     mehamn_lon, norwegian_sea_lon, north_sea_lon, nieuwe_waterweg_lon]
y = [yangshan_lat, sea_of_jap_lat, tsugaru_lat, erimomisaki_lat,
stillehavet_lat, transit_ko_at_lat, lawrence_island_lat, chukchi_sea_lat,
wrangel_lat, kotelny_island_lat, laptev_lat, vilkitsky_lat, kara_sea_lat,
     mehamn_lat, norwegian_sea_lat, north_sea_lat, nieuwe_waterweg_lat]

#Interpolate the n points between each node
#output is a list of lon and a list of lat
lat_interp, lon_interp = [], []
for i in range(len(x)-1):
    az12, az21, dist = g.inv(x[i], y[i], x[i + 1], y[i + 1])
    del_s = 11e3 # distance in meters
    points = round(dist/del_s)
    r = g.fwd_intermediate(x[i], y[i],az12,npts=points,del_s=del_s)
    lat_interp.append(y[i])
    lon_interp.append(x[i])
    for lon,lat in zip(r.lons, r.lats):
        lat_interp.append(lat)
        lon_interp.append(lon)
lat_interp.append(y[-1])
lon_interp.append(x[-1])

length_lat = len(lat_interp)

df = pd.DataFrame(lon_interp)
df1 = pd.DataFrame(lat_interp)
```

```
#make delta_dist_km column
#dist = distance in meters
distance = [0]
for i in range(len(lon_interp)-1):
    for j in range(len(lat_interp)-1):
        az12,az21,dist = g.inv(lon_interp[i], lat_interp[j],lon_interp[i+1],
lat_interp[j+1])
        delta_dist_km = dist/1e3
    distance.append(delta_dist_km)

op = pd.DataFrame.from_dict(
    {'delta_dist_km':distance,
        'x': lon_interp,
        'y':lat_interp,
    }
)

op.to_csv('data/arctic_OP.csv')
```

The below code is developed to run the vessels with the technical details equal to the Baseline on the Arctic route. Two experiments are conducted and run separately. Exp1 is the experiment with speed over ground (SOG) equal to the average SOG of the respective baseline vessels. Exp2 is the experiment with voyage time equal to the voyage time of the respective baseline vessels.

```
mmsi = 219018501
op = pd.read_csv('data/arctic_OP.csv')
orgOP = pd.read_csv('data/Baselines/'+str(mmsi)+'_baseline.csv')
op['delta_dist_km'].replace('', np.nan, inplace=True)
op.dropna(subset=['delta_dist_km'], inplace=True)
op.reset_index(inplace=True, drop=True)

#'''
# create sog and sog_km (experiment 1)
for i in range(len(op)):
    op['sog'] = orgOP['sog'].sum()/len(orgOP['sog'])
    op['sog_km'] = op['sog']*constants.KMS_KN
print(op['sog'])
#print(sog_km)

'''
#sog for constant time (experiment 2)
op['sog'] = op['delta_dist_km'].sum() / orgOP['delta_time_s'].sum() /
constants.KMS_KN
op['delta_time_s'] =op['delta_dist_km'] / (op['sog'] * constants.KMS_KN)
#op['sog']

'''
#create delta_time_s
delta_time_s = op['delta_dist_km'] / op['sog_km']
op['delta_time_s'] = delta_time_s
#'''
```

```
dist_tot = op.delta_dist_km.sum()
print(dist_tot)
org_dist = orgOP.delta_dist_km.sum()
print(org_dist)

#ECA North Sea
eca_exists = []
lat = op['y']
lon = op['x']
# max and min lat and lon found at
https://marineregions.org/gazetteer.php?p=details&id=2350
min_lat = 50.9945
max_lat = 61.017
min_lon = -4.4454
max_lon = 12.0059
for i in range(len(op)):
    if min_lat <= lat[i] <= max_lat:
        if min_lon <= lon[i] <= max_lon:
            eca = 1
    else:
        eca = 0
    eca_exists.append(eca)
op['eca_exists'] = eca_exists
#print(eca_exists)


#weather columns set to zero
beaufort = []
for i in range(len(op)):
    beau = 0
    beaufort.append(beau)
op['beaufort'] = beaufort

#find unixtimestamp
timestamp = orgOP['unixtimestamp'][0]
unixtimestamp=[timestamp]
for i in range(1,len(op.delta_time_s)):
    timestamp += op.delta_time_s[i]
    unixtimestamp.append(timestamp)
op['unixtimestamp'] = unixtimestamp
print(op['unixtimestamp'])

time_tot = op.delta_time_s.sum()
print(time_tot)

#create origin column
origin = []
for i in range(len(op)):
    org =1
    origin.append(org)
op['origin'] = origin

op.drop(op.columns[op.columns.str.contains('unnamed',case = False)],axis = 1,
inplace = True)
op.drop(op.columns[op.columns.str.contains('new_timestamp',case =
False)],axis = 1, inplace = True)
```

```
op.to_csv('data/Arctic routes/exp1/'+str(mmsi)+'arctic_exp1.csv')
#op.to_csv('data/Arctic routes/exp2/'+str(mmsi)+'arctic_exp2.csv')
```

Appendix B: Fuel consumption (g/DWT-nm) for vessels in Cv and Ct

The variation in fuel consumption within each operational profile on the Arctic route is marignal. The Ct OP with slowsetaming has the largest reduction in fuel consumption (g/DWT-nm) from the baselne profile. The vessels on Cv with equal median speed as the median speed of the baseline has no change in interquartile fuel consumption from the baseline.

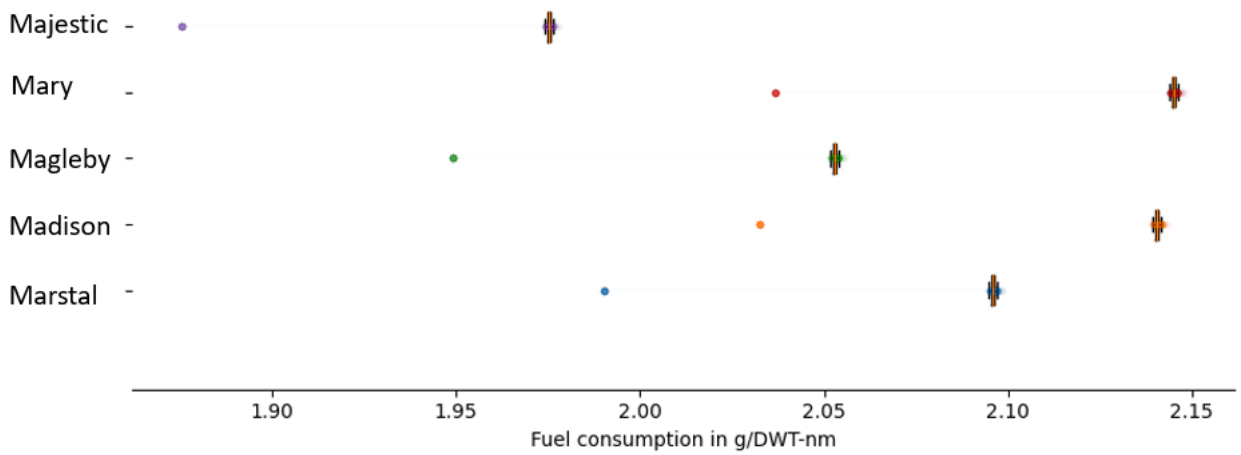

Figure B.1: Variation in fuel consumption (g/DWT-nm) within each Cv OP on the Arctic route

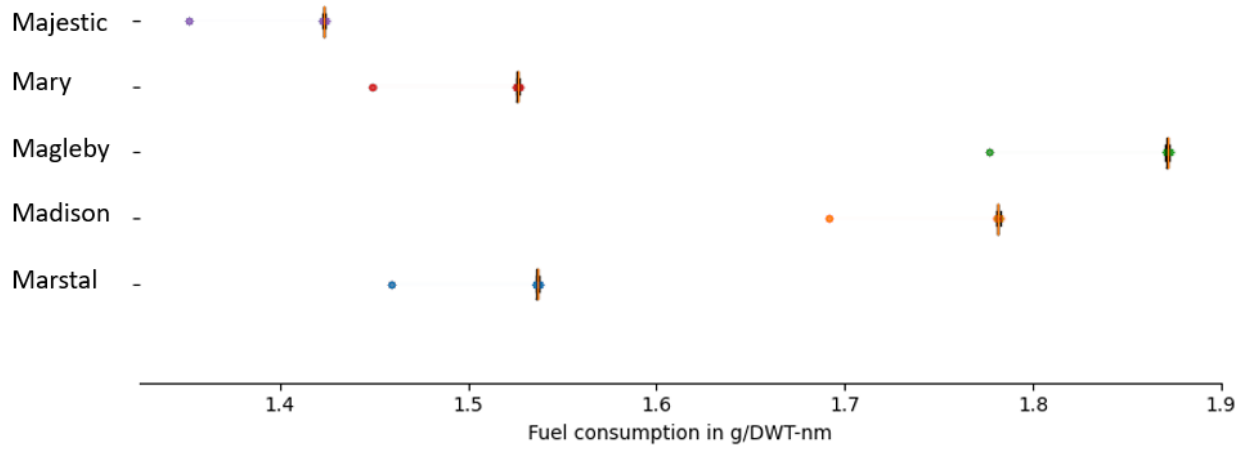

Figure B.2: Variation in fuel consumption (g/DWT-nm) within each Ct OP on the Arctic route

Appendix C: Sum of selected emissions in metric tons

The following tables list the total emissions of CO_2, SO_2, BC, and CH_4 associated with the five case vessels in the baseline, Cv, and Ct simulation. The values are given in metric tons.

Table C.1: CO_2 emissions from the respective experiments in metric tons.

CO_2											
	HFO			MDO		LNG LP			LNG HP		
	Baseline	Cv	Ct	Cv	Ct	Baseline	Cv	Ct	Baseline	Cv	Ct
Marstal	15130.8	13013.8	9795.3	12740.5	9594.5	10447.8	9612.3	7144.7	10559.6	8976.2	6671.9
Madison	14983.2	13254.4	11178.9	12975.5	10946.6	11107.8	9829.5	8117.7	8268.1	9178.7	7580.2
Magleby	13455.9	12747.7	11699.1	12479.8	11455.0	9932.6	9354.6	8470.7	9329.2	8734.9	7909.6
Mary	15316.7	13273.0	9717.9	12993.3	9519.0	11407.5	9843.0	7055.2	10706.8	9191.0	6619.6
Majestic	14025.9	12300.0	9145.4	12042.8	8959.7	10394.0	8923.8	6640.6	9741.4	8333.2	6230.5
Total	72912.5	64588.9	51536.6	63231.9	50474.8	53289.7	47563.3	37428.8	48605.0	44414.1	35011.8

Table C.2: SO_2 emissions from the respective experiments in metric tons.

SO_2											
	HFO			MDO		LNG LP			LNG HP		
	Baseline	Cv	Ct	Cv	Ct	Baseline	Cv	Ct	Baseline	Cv	Ct
Marstal	226.8	195.3	143.3	6.2	4.6	0.1	0.1	0.1	0.1	0.1	0.1
Madison	220.2	199.1	165.8	6.3	5.3	0.1	0.1	0.1	0.1	0.1	0.1
Magleby	202.5	191.0	174.2	6.0	5.5	0.1	0.1	0.1	0.1	0.1	0.1
Mary	228.1	199.4	141.3	6.3	4.6	0.2	0.1	0.1	0.2	0.1	0.1
Majestic	202.8	183.8	131.9	5.8	4.3	0.1	0.1	0.1	0.1	0.1	0.1
Total	1080.5	968.7	756.5	30.6	24.4	0.7	0.5	0.4	0.6	0.5	0.4

Table C.3: BC emissions from the respective experiments in metric tons.

BC											
	HFO			MDO		LNG LP			LNG HP		
	Baseline	Cv	Ct	Cv	Ct	Baseline	Cv	Cv	Baseline	Cv	Ct
Marstal	0.305	0.267	0.238	0.111	0.106	0.005	0.004	0.004	0.004	0.004	0.004
Madison	0.295	0.269	0.250	0.111	0.107	0.005	0.004	0.004	0.004	0.004	0.004
Magleby	0.278	0.264	0.255	0.110	0.108	0.005	0.004	0.004	0.004	0.004	0.004
Mary	0.308	0.269	0.237	0.111	0.106	0.006	0.004	0.004	0.004	0.004	0.004
Majestic	0.289	0.261	0.232	0.109	0.105	0.005	0.004	0.004	0.004	0.004	0.004
Total	1.475	1.329	1.213	0.553	0.532	0.026	0.022	0.021	0.022	0.021	0.021

Table C.4: CH4 emissions from the respective experiments in metric tons.

	CH_4					
	LNG LP			LNG HP		
	Baseline	Cv	Ct	Baseline	Cv	Ct
Marstal	43.7	44.7	63.4	6.3	5.5	7.7
Madison	50.9	43.8	54.6	4.9	5.3	6.7
Magleby	48.7	45.9	51.4	5.9	5.6	6.3
Mary	52.2	43.9	64.1	6.4	5.4	7.8
Majestic	58.0	48.3	67.3	7.1	5.9	8.2
Total	253.5	226.6	300.8	30.7	27.7	36.7

Appendix D: Climate impacts in kg CO_2-equivalnets per transport work

The climate impact is computed by multiplying the kilograms of each emisisons with its respecitve metric value and divided by deadweigth tonnage and distance of the respective voyage.

D.1: Net climate impact per experiment

Table D.1: Net climate impact (kg CO_2-eq./DWT-nm) for the respective operational profiles. The climate impact is calculated for GTP and GWP with a 20 and 100 year time horizon

		GTP100	GTP20	GWP100	GWP20
HFO	Baseline	58.5	-249.8	-15.3	-135.5
	Cv	51.6	-233.9	3.8	-57.4
	Ct	38.4	-166.0	4.3	-39.4
MDO	Cv	55.7	-195.7	21.7	9.5
	Ct	41.4	-138.7	17.0	8.1
LNG LP	Baseline	47.4	-204.3	17.9	21.1
	Cv	40.9	-193.9	13.1	15.5
	Ct	31.3	-126.4	15.4	26.0
LNG HP	Baseline	43.0	-226.0	7.0	-3.9
	Cv	36.9	-211.7	3.9	-5.7
	Ct	27.8	-150.0	4.4	-1.7

D.2: Climate impact per emissions species (GWP)

Table D.2: Climate impact in kg CO_2-eq./DWT-nm (GWP20) for each emission species and the respective operational profiles

GWP20											
	HFO			MDO		LNG LP			LNG HP		
	Baseline	Cv	Ct	Cv	Ct	Baseline	Cv	Ct	Baseline	Cv	Ct
CO_2	71.13	63.26	46.81	61.93	45.86	52.71	45.90	34.15	49.40	42.86	32.04
N_2O	1.01	0.92	0.66	0.89	0.64	0.98	0.89	0.64	0.98	0.89	0.64
CH_4	0.00	0.00	0.00	0.00	0.00	24.51	20.71	28.86	2.99	2.53	3.52
NO_x	-53.67	-49.74	-35.62	-49.74	-35.62	-53.67	-49.74	-35.62	-53.85	-49.74	-35.80
SO_2	-154.29	-73.33	-52.63	-2.35	-1.74	-0.09	-0.04	-0.03	-0.09	-0.04	-0.03
BC	3.55	3.60	3.21	0.87	0.83	0.06	0.06	0.06	0.06	0.06	0.06
OC	-3.60	-2.42	-2.22	-2.42	-2.22	-3.60	-2.42	-2.22	-3.60	-2.42	-2.23
CO	0.37	0.27	0.36	0.27	0.36	0.20	0.18	0.13	0.16	0.14	0.10

Table D.3: Climate impact in kg CO_2-eq./DWT-nm (GWP100) for each emission species and the respective operational profiles

GWP100											
	HFO			MDO		LNG LP			LNG HP		

	Baseline	Cv	Ct	Cv	Ct	Baseline	Cv	Ct	Baseline	Cv	Ct
CO_2	71.13	63.26	46.81	61.93	45.86	52.71	45.90	34.15	49.40	42.86	32.04
N_2O	1.01	0.92	0.66	0.89	0.64	0.98	0.89	0.64	0.99	0.89	0.64
CH_4	0.00	0.00	0.00	0.00	0.00	8.38	7.08	9.86	1.02	0.86	1.20
NO_x	-43.28	-40.11	-28.72	-40.11	-28.72	-43.28	-40.11	-28.72	-43.43	-40.11	-28.87
SO_2	-44.23	-20.71	-14.86	-0.66	-0.49	-0.03	-0.01	-0.01	-0.02	-0.01	-0.01
BC	0.97	1.01	0.90	0.24	0.23	0.02	0.02	0.02	0.02	0.02	0.02
OC	-0.98	-0.68	-0.62	-0.68	-0.62	-0.98	-0.68	-0.62	-0.98	-0.68	-0.62
CO	0.12	0.09	0.12	0.09	0.12	0.06	0.06	0.04	0.05	0.05	0.03

D.3: Climate impact per emissions species (GWP)

Table D.4: Climate impact in kg CO2-eq./DWT-nm (GTP20) for each emission species and the respective operational profiles

GTP20											
	HFO			MDO		LNG LP			LNG HP		
	Baseline	Cv	Ct	Cv	Ct	Baseline	Cv	Ct	Baseline	Cv	Ct
CO_2	71.13	63.26	46.81	61.93	45.86	52.71	45.90	34.15	49.40	42.86	32.04
CH_4	0.00	0.00	0.00	0.00	0.00	19.84	16.76	23.36	2.42	2.05	2.85
N_2O	1.08	0.98	0.70	0.95	0.68	1.05	0.95	0.68	1.05	0.95	0.68
NO_x	-276.99	-256.70	-183.83	-256.70	-183.83	-276.99	-256.70	-183.83	-277.94	-256.70	-184.77
SO_2	-45.26	-41.60	-29.85	-1.32	-0.98	-0.03	-0.02	-0.02	-0.03	-0.02	-0.02
BC	1.03	0.94	0.84	0.23	0.22	0.02	0.02	0.02	0.02	0.01	0.02
OC	-1.04	-0.96	-0.88	-0.96	-0.88	-1.04	-0.96	-0.88	-1.05	-0.96	-0.88
CO	0.23	0.17	0.23	0.17	0.23	0.12	0.11	0.08	0.10	0.09	0.06

Table D.5: Climate impact in kg CO2-eq./DWT-nm (GTP100) for each emission species and the respective operational profiles

GTP100											
	HFO			MDO		LNG LP			LNG HP		
	Baseline	Cv	Ct	Cv	Ct	Baseline	Cv	Ct	Baseline	Cv	Ct
CO_2	71.13	63.26	46.81	61.93	45.86	52.71	45.90	34.15	49.40	42.86	32.04
CH_4	0.00	0.00	0.00	0.00	0.00	1.26	1.07	1.49	0.15	0.13	0.18
N_2O	0.90	0.81	0.58	0.79	0.57	0.87	0.79	0.57	0.87	0.79	0.57
NO_x	-7.27	-6.74	-4.83	-6.74	-4.83	-7.27	-6.74	-4.83	-7.30	-6.74	-4.85
SO_2	-6.27	-5.77	-4.14	-0.18	-0.14	0.00	0.00	0.00	0.00	0.00	0.00
BC	0.13	0.12	0.11	0.03	0.03	0.00	0.00	0.00	0.00	0.00	0.00
OC	-0.13	-0.12	-0.11	-0.12	-0.11	-0.13	-0.12	-0.11	-0.13	-0.12	-0.11
CO	0.02	0.01	0.02	0.01	0.02	0.01	0.01	0.01	0.01	0.01	0.01

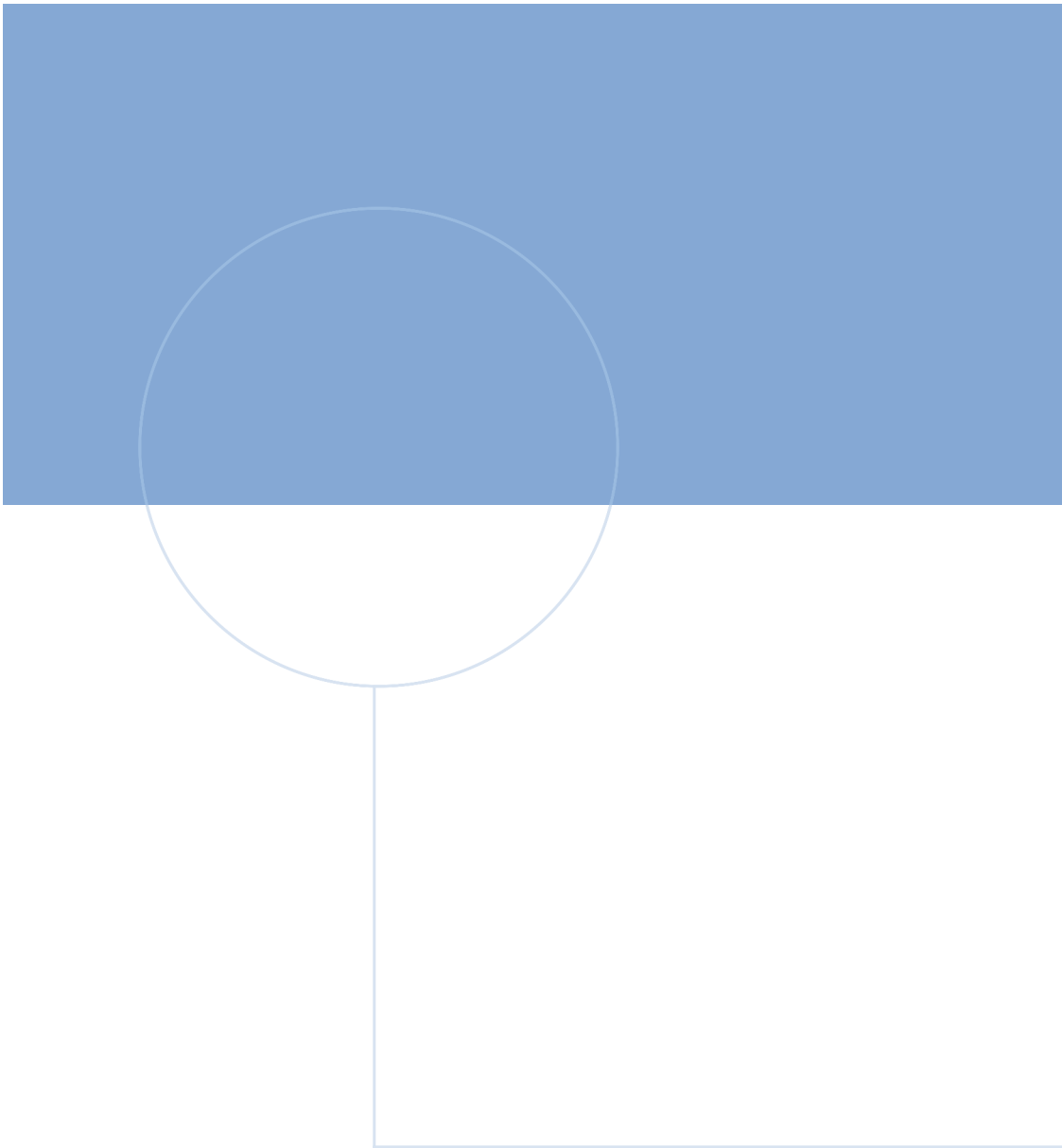

NTNU

Norwegian University of
Science and Technology